ANNUAL REVIEWS

Annual Review of Cell and Developmental Biology

The Unreasonable Effectiveness of Reaction Diffusion in Vertebrate Skin Color Patterning

Michel C. Milinkovitch, Ebrahim Jahanbakhsh, and Szabolcs Zakany

Laboratory of Artificial and Natural Evolution, Department of Genetics and Evolution, University of Geneva, Geneva, Switzerland; email: Michel.Milinkovitch@unige.ch

ANNUAL REVIEWS **CONNECT**

www.annualreviews.org

- Download figures
- Navigate cited references
- Keyword search
- Explore related articles
- Share via email or social media

OPEN ACCESS (cc) BY

Keywords

reaction diffusion, Turing patterns, skin color patterns, cellular automata, phenomenological models, sequential patterning

Abstract

In 1952, Alan Turing published the reaction-diffusion (RD) mathematical framework, laying the foundations of morphogenesis as a self-organized process emerging from physicochemical first principles. Regrettably, this approach has been widely doubted in the field of developmental biology. First, we summarize Turing's line of thoughts to alleviate the misconception that RD is an artificial mathematical construct. Second, we discuss why phenomenological RD models are particularly effective for understanding skin color patterning at the meso/macroscopic scales, without the need to parameterize the profusion of variables at lower scales. More specifically, we discuss how RD models (*a*) recapitulate the diversity of actual skin patterns, (*b*) capture the underlying dynamics of cellular interactions, (*c*) interact with tissue size and shape, (*d*) can lead to ordered sequential patterning, (*e*) generate cellular automaton dynamics in lizards and snakes, (*f*) predict actual patterns beyond their statistical features, and (*g*) are robust to model variations. Third, we discuss the utility of linear stability analysis and perform numerical simulations to demonstrate how deterministic RD emerges from the underlying chaotic microscopic agents.

Contents

1. INTRODUCTION

1.1. Alan Turing

Alan M. Turing (1912–1954) was undoubtedly one of the greatest scientists of the twentieth century. His research was pivotal in computer science as he formalized the concepts of a computer algorithm and of a Turing machine (i.e., an automaton able to implement any algorithm). Turing's initial theoretical work, as well as circuit and memory design by John von Neumann, led to the development of the first programmable electronic general-purpose digital computers. Turing made other key contributions to logic and computer science, and he is arguably (again, together with John von Neumann) the founder of artificial intelligence. Notably, Turing worked for the British code-breaking center in Bletchley Park during World War II, and he led the famous Hut 8 section that improved Polish special-purpose machines, eventually breaking the German naval Enigma cipher, thereby shortening the war and saving countless lives. Turing's contribution to modern cryptoanalysis is probably what made him most famous in the public eye, although this public recognition occurred many years after his death as most of his research and discoveries in that field remained a British state secret until 2012.

In 1951, Turing became interested in morphogenesis, i.e., how living organisms develop their shape and form. He had the remarkable intuition that morphogenesis might emerge from simple physicochemical first principles that could be described mathematically. In 1952, he published a masterpiece article (Turing 1952) establishing the reaction-diffusion (RD) mathematical framework[1] in which concentrations of two (or more) diffusing[2] and reacting molecular species (RD

---

[1] In the framework of population genetics, Ronald Fisher as well as Andrey Kolmogorov, Ivan Petrovskii, and Nikolai Piskunov previously introduced an RD equation (Fisher 1937, Kolmogorov et al. 1937) with only one component (the frequency of an allele): The resulting dynamics can exhibit front propagation but not a stationary pattern.

[2] As discussed in **Supplemental Appendix 4.7**, spatial symmetry breaking due to Turing instability requires a minimum of two morphogens, which must also diffuse at different effective rates. Periodic spatial patterning

components) are computed through time and space and form temporal and/or spatial patterns. Turing reflected, long before modern cell and molecular developmental biology, that spatial patterning of these chemical morphogens could then be translated into forms; i.e., it would lead to morphological patterning. Turing died a few days before turning 42, shortly before completing another mathematical biology article on phyllotaxis, i.e., lateral-organ spatial arrangements in plants.

1.2. Objectives of This Review

As we elaborate on in Section 2, it is clear today that skin color patterning in vertebrates consists of the symmetry-breaking self-organizational spatial segregation of chromatophores during development through short- and long-range cell–cell interactions that can be efficiently described at the continuum limit with partial differential equations (PDEs) in Alan Turing's RD framework. The terminology and jargon in the previous sentence illustrate that the concepts of biological self-organized patterning are deeply rooted within dynamical systems theory (arguably founded by the work of the polymath Henri Poincaré at the brink of the twentieth century), a field of mathematics that became hugely important in modern physics. Unfortunately, the teaching of dynamical system theory is absent in most biology curricula, possibly explaining that fundamental self-organizational concepts, such as RD, are still viewed today with suspicion by a substantial proportion of developmental biologists. This cultural gap between biology and physics might explain why Turing's RD framework, despite its foundational and groundbreaking nature, was ignored for 20 years after its publication, before it was promoted by Alfred Gierer and Hans Meinhardt (Gierer & Meinhardt 1972, Meinhardt & Gierer 1974). After three more decades of being largely ostracized in developmental biology due to philosophical and historical reasons (reviewed in Green & Sharpe 2015), Turing's concept of RD as a genuine and fundamental morphogenetic patterning mechanism recently experienced a highly deserved revival.

Instead of exhaustively reviewing the literature on RD [several excellent reviews are already available on the topic (e.g., Cross & Hohenberg 1993, Epstein & Xu 2016, Green & Sharpe 2015, Kondo & Miura 2010, Kondo et al. 2021, Murray 2003, Schweisguth & Corson 2019)], the present article aims to mitigate the misunderstanding between reductionists and phenomenologists. The former, who currently dominate in number in the field of developmental biology, aim at describing the most intricate molecular details of gene expression and signaling underlying patterning, whereas the latter (smaller) crowd favors effective models that ignore much of the underlying molecular details (Milinkovitch 2021). We view these two approaches as complementary.

Our specific objectives in this review are threefold. First, we summarize in **Supplemental Appendix 1** our perception of Turing's line of thought—as with many foundational pieces of work, Turing's (1952) article is very much cited but rarely read. We think that highlighting Turing's central focus on the biological question of morphogenesis (as a symmetry-breaking process grounded in first principles) can help alleviate the misconception that RD is an artificial mathematical construct irrelevant to the real world. We also stress the outstanding vision of Turing, not only in identifying and formalizing the dominating principles of chemical-based self-organized morphogenesis, but also regarding the limitations and future perspectives of his theory. We strongly advise readers not to skip **Supplemental Appendix 1** as it greatly helps with understanding the main text.

Second, we discuss in Section 2 how RD became recognized as remarkably efficient for describing the diversity and complexity of skin color patterning, hence the title of this review.

---

with a single morphogen (Wang et al. 2022) or with two morphogens exhibiting identical diffusion coefficients (Marcon et al. 2016) has been recently claimed. However, both models integrate an additional nondiffusing morphogen. We argue that the full set of concentrations should be considered when evaluating diffusion asymmetry. In both studies, this asymmetry is large as one of the two (or more) RD components is nondiffusive.

Mathematicians and physicists will recognize that our title is inspired by the famous 1959 New York lecture [published 1 year later (Wigner 1960)] by the Nobel Prize laureate Eugene Wigner, titled "The Unreasonable Effectiveness of Mathematics in the Natural Sciences." The effectiveness of mathematics in science remains a puzzle "bordering on the mysterious" (Wigner 1960, p. 2) that will undoubtedly keep philosophers busy for a long time. The effectiveness of RD is admittedly less grandiose, but we discuss in Section 2.1 how it started to be seriously considered when Hans Meinhardt and Alfred Gierer at the Max Planck Institute in Tübingen, as well as James Murray at the University of Oxford, demonstrated that RD computer simulations recapitulate the diversity of skin patterns observed in real animals (Gierer & Meinhardt 1972; Meinhardt & Gierer 1974; Murray 1980, 1981a,b). In Section 2.2, we illustrate that the unreasonable effectiveness of RD in vertebrate skin color patterning originates from two main sources: (*a*) contrary to morphogenetic processes generating changes in local tissue geometry, skin color patterning does not require coupling RD with a mechanical model, and (*b*) real-life morphogens diffuse (literally or effectively) and react. Indeed, we argue that phenomenological effective RD models (focusing on the meso/macroscopic scales at which the color pattern occurs) capture most of the underlying dynamical system of cell–cell interactions because these interactions occur through the effective diffusion of morphogens (Romanova-Michaelides et al. 2022)[3] or, more precisely, through short- and long-range cell–cell contacts that can be readily translated into small and large diffusion coefficients. This effective phenomenological approach was championed by Shigeru Kondo and his collaborators at the University of Osaka in Japan. In a series of influential papers (Inaba et al. 2012, Kondo & Asal 1995, Nakamasu et al. 2009, Yamaguchi et al. 2007), Kondo and his team demonstrated that biological experiments (including laser ablation of specific chromatophores) allowed identification of the signs (activation or inhibition) and range (short or long) of the interactions among chromatophores. This led to the reconstruction of a cell–cell interaction network that could then be translated into a simple set of three PDEs (Nakamasu et al. 2009), called hereafter the NTKK-2009 (Nakamasu et al. 2009) model, adeptly recapitulating the skin color patterning process in wild-type and mutant zebrafish morphs, as well as in related species, despite that it does not integrate the interactions involving iridophores (Frohnhofer et al. 2013, Owen et al. 2020, Patterson & Parichy 2013, Singh et al. 2014, Volkening & Sandstede 2018).

RD can reproduce a large diversity of skin color patterns observed in nature (Gierer & Meinhardt 1972; Meinhardt & Gierer 1974; Murray 1980, 1981a,b), from spatially homogeneous to spatially periodic (the so-called Turing patterns) and even time cyclic [i.e., traveling waves (Suzuki et al. 2003)]. In Sections 2.3 to 2.6, we discuss additional aspects of RD effectiveness in vertebrate skin color patterning: Numerical simulations implementing RD in skin domains of nontrivial geometry predict unsuspected emerging patterns and dynamics. In Section 2.3, we elaborate on the effects of tissue size and shape [touched upon early on by Murray (1981a,b)] on RD patterning, as well as conditions that can lead to ordered sequential patterning. In particular, we examine how mild extensions of the simple two-morphogen RD system can generate new rich and spectacular (but poorly studied) behaviors that are likely involved in key biological morphogenetic processes, such as animal segmentation.

We then present in Section 2.4 the recent and surprising realization (Fofonjka & Milinkovitch 2021, Jahanbakhsh & Milinkovitch 2022, Manukyan et al. 2017, Zakany et al. 2022) that the superposition of RD with periodic variation of skin geometry (in the form of reptilian skin scales) can

---

[3]Note that effective diffusion can involve multiple processes such as binding/unbinding to receptors, intracellular recycling, and transcytosis. Hence, the reader might find it useful to substitute the term effective diffusion by range of action.

generate spatial discretization of the pattern, as well as cellular automaton (CA) (von Neumann 1951) or Lenz-Ising (Ising 1925, Lenz 1920) dynamics of the patterning process. These results illustrate how effective phenomenological models can readily integrate new geometrical parameters and efficiently capture these unexpected dynamics without the need to parameterize the unmanageable profusion of variables at the nanoscopic and microscopic scales (Milinkovitch 2021).

Section 2.5 outlines how RD predicts actual patterns beyond their statistical features and how natural selection tends to keep skin color patterning (and probably many other self-organizational processes in actual biological systems) out of the chaotic regime, hence making its trajectories largely predictable (Jahanbakhsh & Milinkovitch 2022). We also illustrate in Section 2.5 that RD not only predicts the CA-like scale-by-scale color patterning of the skin in multiple lizard species but also predicts unsuspected and subtle color subclustering that correlates with the colors of the scales' neighbors. We then show in Section 2.6 that, irrespective of their form, discretization, and spatial dimensionality, phenomenological RD models are highly robust in predicting multiple features of the skin color patterning process. It is our hope that the results summarized in Sections 2.1–2.6 will convince the reader that RD should not be viewed with suspicion despite our lack of knowledge regarding the relevant activator and inhibitor molecules. Indeed, we conjecture that the identity of these molecular actors is mostly irrelevant if one aims to understand the meso/macroscopic behavior of the dynamical system (Milinkovitch 2021).

Third, we provide more technical information in the **Supplemental Appendices**. In **Supplemental Appendix 2**, we describe the original NTKK-2009 model as well as an extension of it that we use to model traveling waves of patterning. In **Supplemental Appendix 3**, we describe conditions that generate the combined expression of stationary Turing patterns and sustained oscillations leading to sequential patterning, a combination that may be involved in somitogenesis (as discussed in Section 2.3).

We then discuss in **Supplemental Appendix 4** the very convenient fact that RD is amenable to linear stability analysis. Because complexity-generating RD systems are fundamentally nonlinear, their behavior cannot, generally, be assessed analytically and must be, instead, investigated through cumbersome and computer-intensive numerical simulations. Fortunately, linearized RD equations allow us to quickly specify the range of RD parameter values that will lead to temporal or spatial patterns. Numerical simulations can then be restricted to this so-called Turing space. Linear stability analysis is technical; the less mathematically inclined reader can omit it as it is not required to understand any of the other sections of this review.

Finally, we discuss in **Supplemental Appendix 5** the advantages of the deterministic nature of the RD mathematical model. Indeed, biological pattern formation processes are deterministic because they are unlikely to involve quantum mechanical effects. This does not necessarily mean that they are fully predictable, as the nonlinearity of interactions among components can make the dynamical system highly sensitive to initial conditions—this is the essence of deterministic chaos (Lorenz 1963). However, despite the auspicious results summarized in Section 2, using a deterministic model might seem counterintuitive because of the unpredictability of reactions and diffusion at the microscopic scale. To alleviate this (spurious) concern, we perform, in **Supplemental Appendix 5**, numerical simulations recapitulating the microscopic molecular collisions required for both molecular diffusion and chemical reactions. We show that deterministic macroscopic spatial patterning emerges from such a microscopic system of interactions, even though the exact behavior of individual particles cannot be predicted; i.e., we show that macroscopic fluctuations tend toward zero when the number of microscopic particles is increased. We are confident that these numerical experiments will help illustrate how deterministic RD (described by Turing's PDEs)—as well as a substantial dose of predictability (see Section 2.5)—emerges at

the continuum limit (i.e., at the meso- and macroscales) despite the chaotic, seemingly stochastic, behavior of the underlying microscopic agents. This demonstration also helps to appreciate the highly counterintuitive contribution of diffusion to RD patterning: Although diffusion (when taken in isolation) is a homogenizing force, it can drive instabilities (hence, patterning) in the context of reacting morphogens whose diffusivities differ. We hope this exercise emphasizes the validity of first-principle thinking, which is at the basis of the mathematical simplicity and elegance of Turing's equations. In essence, our demonstration, grounded in nonequilibrium physics (Prigogine 1955), is comparable to simpler and more familiar equilibrium thermodynamics in which deterministic macroscopic quantities (such as the temperature and pressure of a gas in a container) emerge from the microscopic and chaotic collisions of molecules. **Supplemental Appendix 5** is technical and can be omitted by readers ready to take our word for it.

We end this review with some conclusions in Section 3.

2. THE UNREASONABLE EFFECTIVENESS OF REACTION DIFFUSION IN SKIN COLOR PATTERNING

2.1. Reaction Diffusion Recapitulates the Diversity of Skin Color Patterns Observed in Real Animals

Skin color and color patterns vary extensively among species and populations and play crucial adaptive functions associated with thermoregulation, photoprotection, camouflage, mimicry, and visual communication (Kronforst et al. 2012, Olsson et al. 2013, Protas & Patel 2008, Stuart-Fox & Moussalli 2008, Teyssier et al. 2015). Fishes, amphibians, and squamates (lizards and snakes) exhibit a particularly spectacular range of colors, essentially generated by three types of neural crest–derived chromatophore cells (Bagnara & Matsumoto 2006, Kuriyama et al. 2006, Saenko et al. 2013, Singh & Nüsslein-Volhard 2015, Ullate-Agote et al. 2020): (*a*) melanophores, which produce brown/black melanins; (*b*) xanthophores and erythrophores that, respectively, contain yellow and red pteridine/carotenoid pigments; and (*c*) iridophores that contain quasi-ordered arrays of guanine inclusions, forming 3D photonic crystals that generate structural coloration through light interference. The spatial arrangement of these three cell types produces a variety of patterns (such as stripes, spots, and labyrinths) but also a broad range of colors through nontrivial optical interactions. In other words, the challenge of understanding a specific skin color pattern corresponds to elucidating the developmental mechanisms that establish the spatial variation of chromatophore combinations.

After Hans Meinhardt and Alfred Gierer at the Max Planck Institute in Tübingen reexamined Turing's RD mathematical framework (Gierer & Meinhardt 1972, Meinhardt & Gierer 1974), James Murray at the University of Oxford proposed RD as a universal pattern formation mechanism for animal coat markings (Murray 1980, 1981a,b) on the basis that RD computer simulations recapitulate the diversity of skin patterns observed in real animals. The application of RD mathematical models to the question of skin color patterning had an obvious practical appeal to scientists: Besides being readily observable in real animals, the skin can be approximated as a plane. Hence, most numerical simulations have been performed in two dimensions, avoiding the much heavier computational cost of 3D simulations.

Murray observed that RD also accounts for the spatial variation of patterns on different body parts with different sizes and geometries. He illustrated the effect of domain geometry on the steady-state motifs by the gradual transformation, on the tail of many species, of spots into circular bands (i.e., rings around the circumference of the tail). Although Murray used a tapered planar domain for numerical convenience, his argument remains valid on the surface of a cone. **Figure 1** shows RD numerical simulations with a model generating spots on the plane. We show
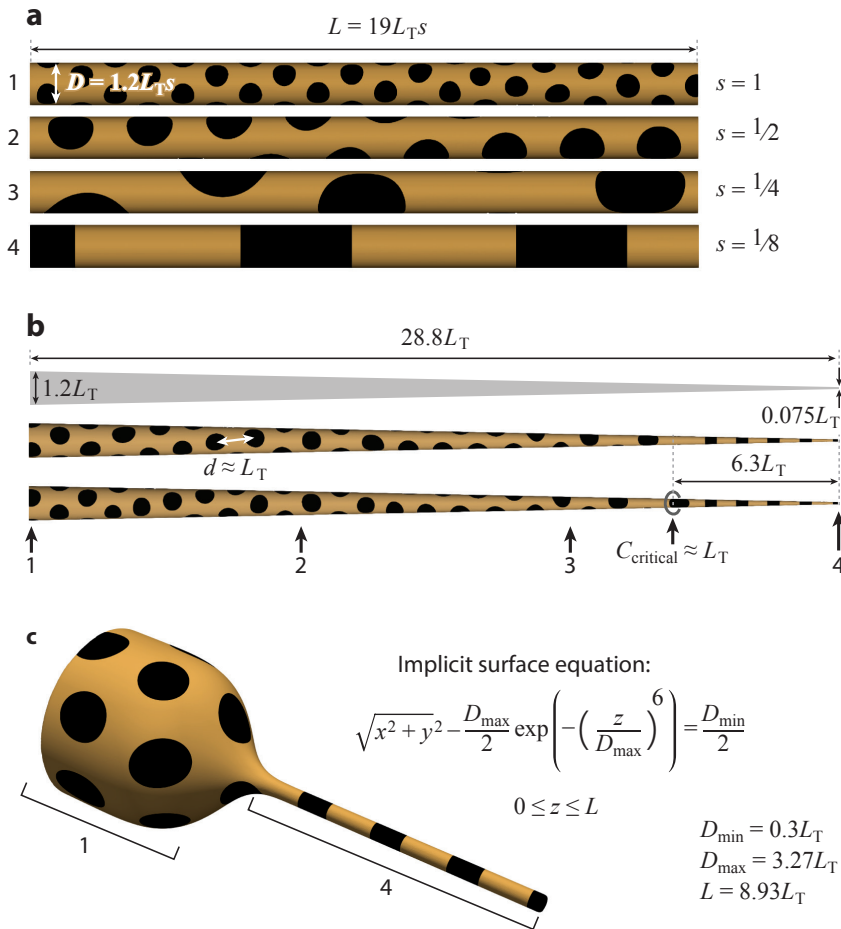
Figure 1

Effect of geometry on RD patterns generated on 3D surfaces. (*a*) Four modes generated with the same NTKK-2009 RD model on cylinders of different sizes. We perform successive reductions of the cylinder diameter by a scale factor *s* but show, for convenience, all cylinders at the same size. All other parameters, including the ratio of diffusion coefficients ($D_w = 12D_{u,v}$), are as in Manukyan et al. (2017), except for $c_v = 0.03$ in order to obtain a spotted (instead of a labyrinthine) pattern on the plane. (*b*) The same transitions among the four modes shown in panel *a* observed along a cone of decreasing diameter. The correspondence between the four diameter values on the cone and the four sets of diffusion coefficients used in panel *a* is shown. *d* represents the pattern length scale, which is approximately equal to the analytical Turing length scale L_T (see **Supplemental Appendix 4** on stability analysis); $C_{critical}$ refers to the critical circumference at which the pattern switches from spots to bands. (*c*) Abrupt shift from mode 1 to mode 4 between the body and tail. All geometrical parameters are represented respective to L_T. Abbreviation: RD, reaction diffusion.

the different modes obtained on cylinders of different sizes (**Figure 1*a***). Similarly, we observe, on a 3D surface conical domain (**Figure 1*b***), the successive transitions among the four modes of **Figure 1*a***. Note also how the spots abruptly transition to bands when the circumference (*C*) of the tail becomes smaller than a critical value ($C_{critical}$); i.e., a 2D pattern (spots) transforms into a 1D pattern (bands) because there is not enough space for accommodating both the circular boundary of a spot and its surrounding inhibitory region in the angular direction of the tail. As

the size of the spot is defined by the arbitrary threshold of the morphogen concentration at which we choose to show black instead of yellow, C_{critical} is better defined as a function of the intrinsic pattern length scale d. We reason that C_{critical} must be $\leq d$ because as two motifs do not merge (by definition) at a distance d, there is no reason for one motif to merge with itself in the direction of the circumference if $C_{\text{critical}} > d$. This relation can be derived more formally from linear stability analysis on the cylinder (Murray 1981a) and is confirmed by our numerical simulations (**Figure 1***b*). In real animals, as the tail is typically conical, the observed pattern can indeed exhibit a shift between successive modes (as in **Figure 1***b*). Alternatively, because the connection between the body and the tail can correspond to a sharp transition in geometry, the pattern can abruptly shift from the first spotted mode on the body to rings around the tail (as in **Figure 1***c*), while intermediate modes are skipped. The former case is observed in the leopard (*Panthera pardus*), jaguar (*Panthera onca*), and cheetah (*Acinonyx jubatus*), whereas the latter is observed in genets (genus *Genetta*). Although the final pattern observed in the adult depends on the tail geometrical parameters, i.e., length and angle of tapering at the embryonic stage at which the patterning takes place, there are logical constraints that exclude some solutions; e.g., if the patterning processes in the body and tail are the same (i.e., they involve the same molecular interactions and effective parameters, and occur approximately at the same time), it is impossible to produce a striped animal with a spotted tail.

Clearly, the early simulations performed by Hans Meinhardt and Alfred Gierer as well as by James Murray convincingly demonstrate that RD has the capacity to qualitatively recapitulate the diversity of skin color patterns observed in nature. However, as appealing and persuasive as all these observations can be, they have sometimes been deemed inconclusive because other (non-RD) more intricate self-organizational patterning mechanisms (Cross & Hohenberg 1993) could arguably generate similar patterns. However, in the absence of mechanics and/or advection, such alternatives to RD have not been explicitly proposed to date.

2.2. Cell Biology Validates Reaction Diffusion as an Effective Description of Skin Color Patterning

It is arguably Christiane Nüsslein-Volhard and her collaborators at the Max Planck Institute in Tübingen and Shigeru Kondo and his collaborators at the University of Osaka who kick-started the difficult, sometimes heated, dialog between reductionists and phenomenologists on the mechanisms of skin color patterning. Early reports suggested that skin color patterns in amphibians originated from cell–cell and cell–substrate interactions (Epperlein & Claviez 1982, Epperlein et al. 1996, Macmillan 1976, Parichy 1996, Twitty 1945). However, it was the selection of a small Asian freshwater Cyprinidae, the zebrafish, as an experimental system (Nüsslein-Volhard 1994, Streisinger et al. 1981) that unleashed a profusion of elegant developmental genetic studies investigating the molecular and cellular mechanisms underlying the interactions among chromatophores that produce the zebrafish's characteristic pattern of longitudinal dark blue and yellow stripes on both the body and fins (e.g., Eom et al. 2015, Frohnhofer et al. 2013, Maderspacher & Nüsslein-Volhard 2003, Mahalwar et al. 2014, Parichy 2003, Parichy & Turner 2003, Patterson & Parichy 2019, Patterson et al. 2014, Singh & Nüsslein-Volhard 2015, Singh et al. 2014). These studies, as well as in vitro analyses (Inaba et al. 2012, Yamanaka & Kondo 2014), indicated that the interactions among melanophores, xanthophores, and iridophores occur not via diffusing molecules but through cell-cell contacts. This result is illustrated by modifications in the wild type, or rescue in color pattern mutants, of the zebrafish skin stripes, through controlled (mis)expression of genes (e.g., *cx41.8* or *igsf11*) whose products mediate chromatophore adhesive interactions (Eom et al. 2012, Watanabe & Kondo 2012).

At first sight, all these results might sound incompatible with a Turing mechanism that requires short-range but also long-range interactions through slow- and fast-diffusing morphogens. Indeed, how could cell-cell contacts occur at long ranges? This conundrum was solved by the group of David Parichy then at the University of Washington, Seattle, that discovered a class of very thin and fast cellular projections (called airinemes) that allow xanthophores to signal to melanophores at long distances, i.e., several cell lengths (Eom et al. 2015). Melanophores also send long projections that interact with xanthophores through Delta-Notch signaling (Hamada et al. 2014). Note that the RD framework additionally requires the signal transferred by airinemes to be diffusive, at least in first approximation. While it is relatively easy to describe the random displacement of cells as a short-range diffusion, it is much more difficult to envision an autonomous random (i.e., diffusive) displacement of airineme tips. The answer to this question came from the remarkable discovery of macrophage-like cells responsible for the production, displacement, and delivery of airinemes emerging from xanthophores (Eom & Parichy 2017). Indeed, xanthophores produce surface blebs (i.e., small, rounded outgrowths) that are identified, via phospholipid phosphatidyl-serine signaling, and engulfed by macrophages. A bleb will then become a vesicle while maintaining a thin connection (the airineme) with the xanthophore. Hence, the vesicle is dragged by the subsequent displacement of the macrophage, and the airineme tethers the vesicle to the originating xanthophore. The airineme extends as the macrophage moves around until the vesicle is spat out and deposited on the surface of a melanophore. As the displacements of macrophages are seemingly random, the corresponding long-range interactions can be deemed a diffusive process at the continuum limit. Therefore, although several molecular actors involved in cell–cell and cell–substrate interactions undoubtedly remain undiscovered, the signaling identified so far for skin color patterning is diffusive (because of the somewhat random displacements of chromatophores and airinemes), and can be appropriately modeled in the RD framework. Note that computational models that explicitly integrate protrusion-mediated signaling have been shown to produce spatial patterns (Vasilopoulos & Painter 2016).

As an alternative to identifying the exact molecular components involved in the interaction network among chromatophores, Kondo and his collaborators took a phenomenological approach that proved to be very effective. Whereas Murray highlighted the similarities between RD-generated patterns and those observed in animals, Kondo & Asal (1995) went one step further by studying the dynamics of the patterning process: They reported that new stripes are steadily intercalated in between existing stripes in the skin pattern of *Pomacanthus* angelfishes as they grow, such that the absolute length scale of the pattern remains invariant. In other words, the pattern does not scale, which is a well-known property of RD patterns; i.e., the length scale of a pattern is not affected by the size of the domain but is an intrinsic feature associated with the set of RD parameter values (see **Supplemental Appendix 4.3** for details on how the length scale is set by the RD parameters, independent of the geometry of the domain). In the same article, the authors also show that the angelfish patterns, especially during the introduction of new stripes, exhibit defects (i.e., branching stripes and unconnected edges) that reorganize following dynamics reminiscent of those observed in RD numerical simulations.

Contrary to the skin color pattern observed in angelfishes, many morphologies do scale with the size of the animal (Barkai & Ben-Zvi 2009). Neither Lewis Wolpert's positional information model (Wolpert 1969, 1971) nor Turing RD patterning mechanisms can, in their traditional forms, explain scaling. Note that, counterintuitively, some growth-controlling morphogens that form a spatial gradient can anyway produce homogeneous growth within an organ. Indeed, elegant molecular analyses (Mateus et al. 2020, Wartlick et al. 2011) have demonstrated that homogeneous growth and growth arrest (Aguilar-Hidalgo et al. 2018) of the fruit fly imaginal disc or the zebrafish

pectoral fin bud are controlled not by the absolute concentrations of the morphogen but by the time derivative (temporal change) of the morphogen concentration within a scaling gradient.

Likewise, RD Turing patterns are not condemned to never scale. Indeed, although the Turing length scale is intrinsic to the RD system, it depends not only on the diffusion constants but also on the reaction function parameters. Hence, any mechanism that would appropriately scale these parameters with the domain size would also make the Turing pattern scale. Such a situation would occur if the reaction rates of a pattern-producing RD system depended on the concentration of an external catalyst produced and degraded on subspaces of appropriate dimensionality (Ishihara & Kaneko 2006). For example, if the catalyst is produced in a fixed subregion of a growing 3D volume and degraded on the surface of that volume, the Turing pattern can scale (for the appropriate model) proportionally to the length (L) of the system. Natural selection is likely able to tune the RD system to produce any kind (e.g., linear) of pattern scaling with domain size. An alternative solution for Turing pattern scaling consists in conserving one quantity in the RD system, for example, the total quantity (i.e., the integrated sum of concentrations) of all RD components in the spatial domain (Ishihara & Kaneko 2006). In that case, the average concentration of this conserved quantity turns out to be an extra parameter (i.e., it is determined by the initial conditions) that affects the pattern length scale. By conservation, the average concentrations of morphogens in three dimensions will scale with the inverse of the domain volume, whereas the scaling factor of the pattern itself will depend on the dimension(s) affected by growth. For example, if the volume grows in only one direction, the pattern will scale (e.g., linearly) in that same direction.

Contrary to both the nonscaling Turing systems (where the pattern is continuously updated during growth) and the scaling Turing systems outlined above, the patterning process can simply become frozen at some point in development. In that case, heterochrony (i.e., differences in the timing and/or rate) in pattern development and arrest can, in principle, account for large differences in pattern length scales among species even if they share exactly the same patterning process. It has been suggested (Bard 1977) that such a mechanism could explain why the plains zebra (*Equus quagga*, formerly *Equus burchellii*) exhibits approximately half the number of stripes in its coat pattern than the Grévy's zebra (*Equus grevyi*): This difference is compatible with a process producing the same pattern length scale and starting at 3 weeks of gestation in both species, but terminating at the third and fifth week of development, respectively. In other words, a pattern fixed earlier in development would produce a smaller number of stripes, and subsequent growth would increase the absolute length scale of the pattern observed in the newborn and adult. More generally, anisotropic growth distorts patterns established earlier in development and can explain discrepancies such as the narrower stripes on body parts (e.g., the head) that exhibit a larger relative size in the embryo than in the adult. This heterochrony hypothesis explaining the patterns observed in different species of zebras has not been confirmed to date because of the difficulties in obtaining zebra embryos, and in performing molecular developmental analyses (e.g., in situ hybridization targeting melanophore precursors) on such large samples.

Evidently, in many cases, genetic mutations affecting RD parameters are responsible for differences in pattern motifs among species, as evidenced by the occasional occurrence of individuals with aberrant patterns, such as spotted zebras or striped cheetahs (Bottriell 1987, Larison et al. 2021). Similarly, it is likely that differences in pattern length scales among closely related species with similar motifs (e.g., stripes) can also be caused by genetic mutations instead of heterochrony. Unfortunately, testing the effects and prevalence of heterochrony and anisotropic growth in nonmodel species is challenging because of both the limited access to embryos (Milinkovitch & Tzika 2007, Tzika & Milinkovitch 2008) and the late development of pigments; i.e., the (pre)pattern is established before it becomes visible. Finally, small differences in initial conditions explain why different individuals of the same species exhibit slightly different patterns, albeit with

identical adaptive statistical features such as the pattern length scale (Jahanbakhsh & Milinkovitch 2022).

Small uncontrolled fluctuations in initial conditions and/or in the developmental process can be considered by using stochastic models, such as the simple two-parameters Lenz-Ising statistical model which describes the patterning process as a time-dependent probability distribution over possible patterns (Zakany et al. 2022). This time dependence manifests as a relaxation towards the thermal equilibrium pattern distribution, characterized by Gibbs entropy maximization at a given mean energy. Remarkably, the (ir)relevance of intraspecific differences then acquires a statistical mechanical interpretation in the framework of the evolutionary process (Zakany et al. 2022). Indeed, patterns with different looks are explored during evolution through the occurrence of genetic mutations, which can affect the link and/or site energies defined in the Lenz-Ising model. Concurrently, the qualitative features of the patterns are subjected to natural selection, which then channels the mean Lenz-Ising energy to a specific value. Despite that the variation of pattern configurations among individuals (i.e., the Gibbs entropy) within the breeding population are maximized at a given Lenz-Ising energy, the evolutionary process is robust because these interindividual differences are virtually irrelevant: Only the mean energy (i.e., the general look of the pattern) matters to selection (Zakany et al. 2022).

Additional observations, simulations, and experiments yet substantially increased the support for an RD system underlying skin color patterning. For example, the hybridization of two East Asian Salmonidae, the white-spotted char (*Salvelinus leucomaenis*) and the black-spotted masu salmon (*Oncorhynchus masou*), generates a hybrid with a labyrinthine pattern (Miyazawa et al. 2010). This result is appreciable as it is compatible with the RD framework: When a specific range of values of a reaction parameter can generate spots of high concentration of one RD component on a background of low concentration, but another specific range of values of the same parameter generates the reverse pattern (antispots, or holes, of low concentration on a background of high concentration), then a labyrinthine pattern can usually be found at intermediate values of that parameter (see **Supplemental Figure 9*b***). In other words, in RD phase space, labyrinthine patterns are usually intercalated between zones with spots and zones with antispots. An extensive phylogenetic analysis of patterns observed in 18,000 fish species suggested that some of the species exhibiting a labyrinthine pattern (e.g., many pufferfishes) originated from hybridization between spotted and antispotted species (Miyazawa 2020). We suggest here that these observations would be especially compatible with effective RD parameters being quantitative traits (i.e., determined by the expression of multiple genes).

RD features related to chromatophore interactions were uncovered through multiple key developmental genetic studies cited above but also in experiments involving in vivo laser ablations of specific chromatophore types. Notably, local ablation of both melanophores and xanthophores is followed by the autonomous regeneration (through chromatophores migrating from surrounding unaffected tissues) of the pattern with rearrangements while keeping the length scale of the original stripes (Yamaguchi et al. 2007), i.e., following dynamics highly similar to those expected from RD. In addition, these ablation experiments enabled identification of the signs (i.e., activation or inhibition) and the range (i.e., short or long) of the interactions between melanophores and xanthophores, thereby providing the experimentally derived phenomenological effective NTKK-2009 RD model (Nakamasu et al. 2009).

2.3. Geometry and Hysteresis Can Have Substantial Impacts on Reaction-Diffusion Patterns

In the case of skin color patterning, the self-organizational process modeled by RD should be deployed on a nontrivial spatial domain given by the geometry of the embryo (or, in some cases,

subsequent stages of development; see Section 2.4). Although the RD process is local, the spatial symmetry breaking that allows for patterns to emerge makes the process sensitive to the geometric features of the spatial domain. This can lead to measurable qualitative phenomena. For example, Murray (1981a,b) noted that the same dominating modes (fixed by the RD system) can produce patterns that look different because of changes in the size and shape of the domain. For example, if the absolute size of the domain in one of its dimensions is smaller than the pattern's intrinsic length scale, then the pattern will manifest itself along the other dimension(s). We already mentioned this property above (see Section 2.1) when discussing the formation of rings around the tail in some species with a spotted body pattern (**Figure 1**). Similarly, in some animals, the presence of a pattern of two distinctive colors separating the body into two parts of the same size, such as the Valais Blackneck (a Swiss domestic breed of goat exhibiting a black front half and a white back half of its body), is explained by the skin domain shape and size at the embryonic time the pattern develops: The length of the animal (from nose to tail) is sufficient to integrate only half a wavelength of the pattern, whereas the circumference of the body is too small for any spatial color pattern to form (**Figure 2a**). Such a case illustrates that, contrary to what is most often implicit in the literature (Čapek & Müller 2019), a simple gradient is not necessarily produced by a localized morphogen source, but it can also be generated through RD.

Murray (1981a,b) extrapolates this reasoning to the zebra's black and white coat pattern: Stripes are oriented along the long axes of both the trunk and the legs. We think that this proposition is incorrect because zebra stripes are patently narrow enough to be incorporated in both directions, even on the legs. We propose that the robust pattern of zebras requires the sequential addition of stripes. To illustrate our point, we perform simulations with an RD model generating stripes with widths similar to those observed in Grévy's zebras. If the simulation is started with small random noise around the homogeneous steady state, the stripes do not exhibit any preferred orientation

(see the left side of **Figure 2b**; **Supplemental Video 1a**). On the other hand, if the initial condition corresponds to an oriented horizontal perturbation, this initial orientation spreads to most of the trunk steady-state pattern (see the middle of **Figure 2b**; **Supplemental Video 1b**). Likewise, if the initial perturbation is oriented vertically (i.e., perpendicular to the trunk's main axis), the steady-state pattern reflects that orientation (see the right side of **Figure 2b**; **Supplemental Video 1c**). Finally, collisions between two or more waves of sequential addition would explain the presence of topological defects on the shoulders of zebras (as well as hips in the Grévy's zebra) (**Figure 2c**; **Supplemental Video 2**).

One remarkable observation deserves further discussion: The vertical stripes of the trunk in plains zebras smoothly transition into horizontal stripes on the back legs (see the middle of **Figure 2c**). Numerical simulations recapitulate such reorientation (see the right side of **Figure 2b**; **Supplemental Video 1c**) that can be understood in terms of signal propagation. Indeed, the pattern forms sequentially from the initial perturbation. The speed of this patterning wave is invariant in all directions (and can be derived from the diffusion coefficients). Hence, each stripe forms as an isoline that corresponds to a specific geodesic distance (from the localization of the initial perturbation), which is identical everywhere along that stripe (**Figure 2d**). This phenomenon is observed both on shapes with zero Gaussian curvature, such as cylinders and cones (**Figure 2d**), and on manifolds with variable curvature, such as tori (**Figure 2e**).

One aspect of RD sequential patterning might be considered rather nonnatural: If the system is in the Turing zone of the parameter space, any small random local perturbation will amplify such that the resulting pattern is more likely to emerge everywhere simultaneously in the form of labyrinthine stripes with no preferred orientation (see left side of **Figure 2b**). To avoid this, the RD components' concentrations must be perfectly homogeneous across the whole spatial domain, except where the initial oriented perturbation is located. This situation is nonnatural because noise

in morphogens' concentrations is likely to occur across the skin. However, much more robust sequential addition processes can take place. For example, one can simply consider the case where the model parameters are such that they are located close to, but still outside of, the Turing zone. In that case, small random perturbations do not cause the emergence of the pattern everywhere, whereas a substantial perturbation can trigger sequential patterning. One such case can be made for the adult zebrafish: Stripes are always horizontal in the wild type because of the initial condition at the onset of pattern development. Indeed, the first adult light interstripe on the body is made of dense iridophores that emerge along the horizontal myoseptum (Frohnhofer et al. 2013),
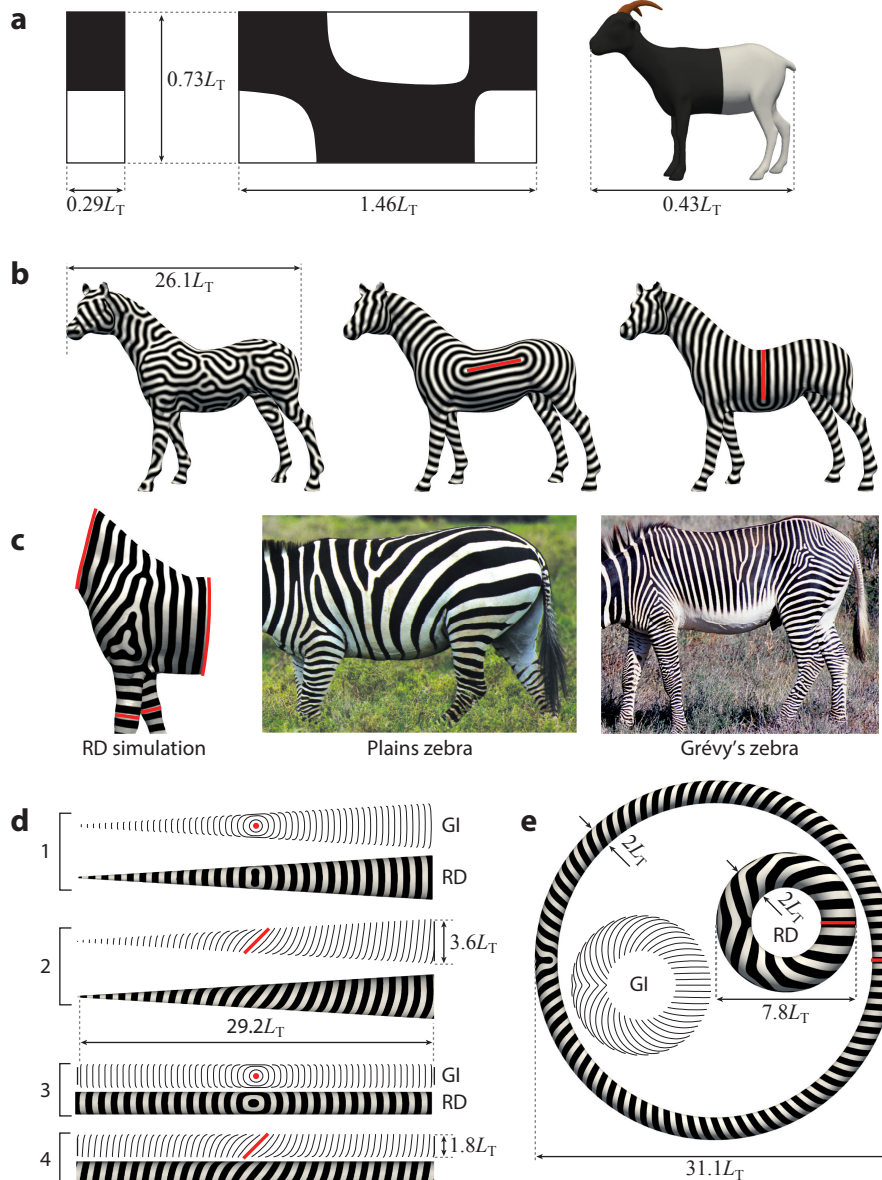
(*Caption appears on following page*)

Figure 2 (*Figure appears on preceding page*)

Effect of geometry on RD striped patterns generated on 3D surfaces. (*a*) Large wavelength striped patterns. The slender cylinder (shown as an unwrapped surface on the *left*) accommodates only the first longitudinal mode of the RD system, resulting in half a wavelength pattern aligned with its main axis. The thicker cylinder (*middle*) is big enough to accommodate two modes (one longitudinal and one angular). A simulation performed on the surface of a goat 3D model (*right*) separates the body into two parts as in the Valais Blackneck real coat pattern. (*b*) Steady-state striped patterns on a zebra 3D model generated with different initial conditions: random perturbations across the whole domain (*left*), a horizontal line of perturbation (*red*) on each flank (*center*), and a vertical line of perturbation around the flanks and back (*right*). The two latter patterns self-organize sequentially (see **Supplemental Video 1b,c**). (*c, left*) RD simulation illustrating how a topological defect on the stripe field can emerge from the collision of three wave fronts propagating from oriented local perturbations. Similar defects are visible on the shoulders of plains zebras (*middle*) as well as shoulders and hips of Grévy's zebras (*right*). Note also that tail bud expansion, which occurs early in development, would explain the oblique orientation of the most posterior body stripes in plains zebras. Photograph of the Grévy's zebra by B. Dupont (CC BY-SA 2.0). (*d*) Numerical simulations illustrating that sequentially patterned stripes self-align perpendicular to the main axis of cones and cylinders. In all cases, RD stripes align to the GIs computed from the initial perturbation. (*e*) Numerical simulations as in panel *c* but on two tori of different sizes. The GIs are shown for the smaller torus. All dimensions are represented respective to the Turing length scale (L_T) of the model [NTKK-2009 with parameters as in Manukyan et al. (2017), except for $c_v = 0.028$ and $c_7 = 0.02$ in order to obtain a striped, instead of labyrinthine, pattern on the plane]. For panels *b–e*, the initial condition is the HSS everywhere except at the initial perturbation (*red*). Abbreviations: GIs, geodesic distance isolines; HSS, homogenous steady state; RD, reaction diffusion.

while melanophores distribute in the skin following different routes (Budi et al. 2008, Dooley et al. 2013). Remarkably, the study of the *choker* mutant confirmed the relevance of this prepattern (Frohnhofer et al. 2013). Indeed, *choker* zebrafishes lack a proper myoseptum because of defects in somite formation, and they exhibit a labyrinthine pattern of stripes; i.e., the stripes are no more predominantly horizontal.

Advocacy for the prevalence of either a prepattern established by the myoseptum or autonomous self-organization has generated exchanges of opposed opinions (Mahalwar et al. 2014, Watanabe & Kondo 2015). However, there is no incompatibility between the two points of view: Initial conditions can substantially impact the resulting steady-state pattern, and they can easily be implemented in numerical simulations. For example, when recapitulating the adult zebrafish pattern, instead of using the classical initial condition of anisotropically distributed random small perturbations, it might be more appropriate to start simulations—in or out of the Turing zone—from a faint horizontal stripe of higher concentration of one of the RD components (to kick-start the general orientation of the pattern). The simple fact that some fish species (e.g., *Danio erythromicron*), that are closely related to the zebrafish, exhibit vertical stripes indicates that the myoseptum is not the only possible directional cue at the onset of adult pattern development. Other, more recent, developmental studies have identified positional information that establishes oriented patterns. For example, somitic mesoderm in birds can control the orientation of yellow and black skin stripes (Haupaix & Manceau 2020, Haupaix et al. 2018).

Another robust sequential addition process can occur through the simultaneous expression of stationary Turing patterns and sustained oscillations (e.g., due to a Hopf bifurcation) discussed above: In some circumstances, they can combine and form a novel emergent patterning mechanism where each new motif is added sequentially in time. For example, such systems have been proposed (Cotterell et al. 2015, Meinhardt 1982) in the context of somitogenesis, as alternatives to the classical clock and gradient model (Baker et al. 2006a,b; Cooke & Zeeman 1976; Richmond & Oates 2012; Soroldoni et al. 2014). As elaborated upon in the **Supplemental Appendix 3.1**, the two sequential addition models of Meinhardt (1982) and Cotterell et al. (2015) are different in form but equivalent in essence, as they both belong to the short-range activation
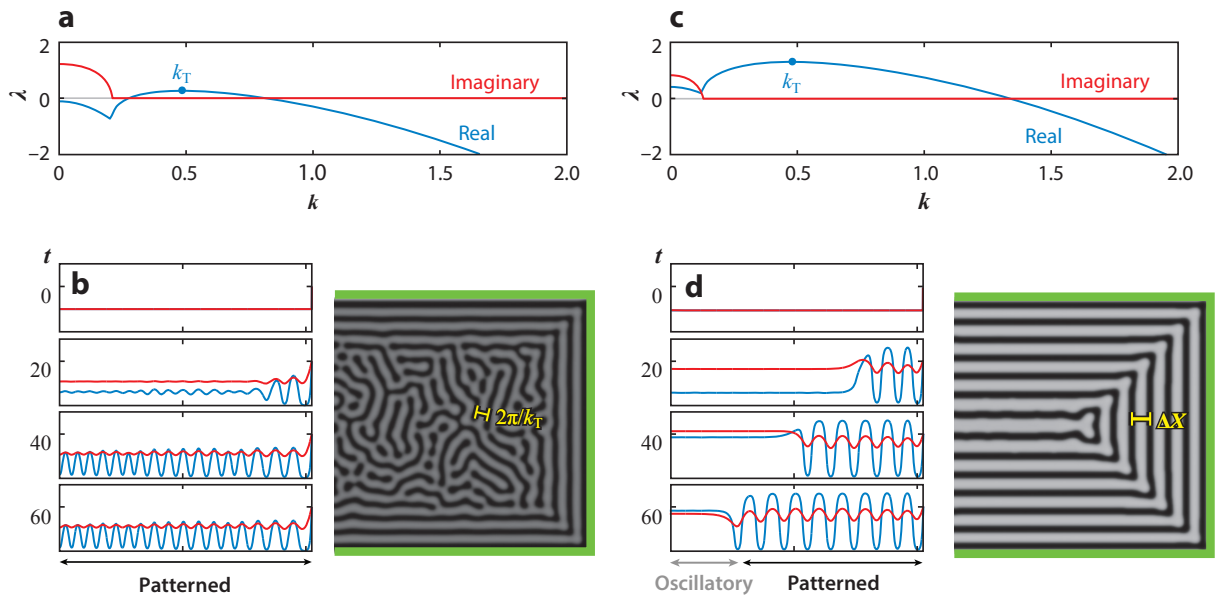
Figure 3

Standard Turing patterning versus sequential patterning with oscillations. (*a*) Linear stability analysis of **Supplemental Equation 3.3** with parameters $K_u = K_v = 0.4$, $w_0 = 0.2$, $D_u = 1$, and $D_v = 30$ around its homogeneous steady state. The growth coefficient $\lambda(k)$ for spatial perturbation with wavenumber k is shown (branch with the largest real part). Since $\mathrm{Re}\lambda(0) \approx -0.1$, the homogeneous steady state is stable but there is a Turing instability: Perturbations with wavenumber $k_T \approx 0.5$ are unstable. (*b, left*) Time evolution of u (*blue*) and v (*red*) for a simulation of this RD system in a 1D domain ($x \in [0, 200]$) with parameters as in panel *a*, showing the emergence of a Turing pattern. Simulation parameters are given in **Supplemental Appendix 6**. (*b, right*) Steady state of u in a 2D simulation (512×512 grid with $\Delta x = 0.5$) with fixed (*three green borders*) or reflecting (*unmarked left border*) boundary conditions. Higher values of u are shown in brighter levels of gray. Turing patterns far from the fixed borders are disordered stripes. (*c,d*) Same as in panels *a* and *b* for $K_u = 0.2$, everything else unchanged. Linear stability analysis in panel *c* shows that the homogeneous steady state is unstable and oscillating, since $\mathrm{Re}\lambda(0) > 0$ and $|Im\lambda(0)| > 0$. As concentrations always stay in the $[0, 1]$ range, it implies the presence of sustained oscillations. A range of perturbations with wavenumber $k_T \approx 0.5$ is even more unstable, indicating that patterns are linearly amplified. Simulation of the RD system in one dimension (*d, left*) shows that oscillations are sustained but patterns are added sequentially until all the domain is patterned. The simulation in two dimensions (*d, right*) shows that patterns with very long-range order are produced. Pattern typical length scales are shown in yellow: It is very close to the Turing length scale $2\pi/k_T$ in panel *b*, whereas its slightly larger value (ΔX) in panel *d* is discussed in **Supplemental Appendix 3**.

plus long-range inhibition category of RD patterning systems. The latter model includes a parameter (here called w_0) that may be interpreted as an external concentration acting as a catalyst for the autoactivation of the activator and/or its interaction with the inhibitor. The parameter w_0 can be set to a constant or it can be prepatterned, e.g., as a spatial gradient. Linear stability analysis shows that, for appropriate choices of parameters, spatial perturbations around a stable homogeneous steady state are amplified; i.e., a Turing instability occurs (**Figure 3a,b**), leading to classical self-organized stable patterning as discussed above. However, other parameter values can be found where both linear amplification of spatial perturbations and sustained oscillations coexist (**Figure 3c,d**). Our numerical simulations in one and two spatial dimensions (**Figure 3d**; **Supplemental Video 3**) show that the compound effect of these two phenomena leads to peculiar patterning dynamics: Each patterning unit is sequentially added next to the previously stabilized unit, while regions that are unpatterned keep oscillating. Each new patterning unit is added after the sustained oscillation has completed a full cycle. In **Supplemental Appendix 3.1**, we propose (*a*) how sustained oscillations and spatial perturbation amplification interact nontrivially in the

Supplemental Material >

nonlinear regime to produce sequential patterning and (*b*) how a spatial gradient of the external concentration w_0 both dispenses for the need for a special boundary condition (e.g., the existence of a first stripe, contrary to the case discussed above for the zebra) and allows for kinematic waves to develop. This latter point is important because spontaneous sequential patterning and kinematic waves are observed in somitogenesis (e.g., in zebrafish), making RD a compelling paradigm for understanding this morphogenetic process as a self-organized phenomenon.

Finally, we note here a nice property of this sequential patterning mechanism: The spatial interval ΔX between pattern units depends to some extent on the period ΔT of the oscillating region (**Supplemental Figure 5e**), which, itself, depends on the value of w_0 (see **Supplemental Figure 5b**). Hence, ΔX determines an extra length scale of self-organization that is distinct from the Turing length scale of the system (**Supplemental Figure 5f**). In other words, changing the oscillation period through variation of w_0 may provide an elegant mechanism for pattern length size control (**Supplemental Figure 5g**) in some systems. Many additional details on sequential patterning with sustained oscillations are available in **Supplemental Appendix 3.1**. Irrespective of the exact process involved, the two types of sequential patterning described above are very efficient at producing highly reproducible patterns ordered on much larger length scales (see the middle and right side of **Figure 2b** and right side of **Figure 3d**) than in the Turing case (see the left side of **Figure 2b** and right side of **Figure 3b**).

The hexagonal lattice of avian feathers and snake latero-dorsal scales is brought about by another type of sequential dynamics: Rows of feather primordia in birds and rows of scale placodes in snakes are added one after the other in spreading waves (Ho et al. 2019, Tzika et al. 2023). The resulting pattern is highly ordered and emerges from dimensionality reduction: The wave front produces a quasi-1D process of placode development along the line separating patterned and unpatterned skin; i.e., each new placode within a new row develops in a quasi-1D manner out of register (i.e., in antiphase) with placodes from the previous row. Additional details on these dynamics, and their molecular determinants, in birds and snakes are provided in **Supplemental Appendix 3.2**.

2.4. Reaction Diffusion and Geometry Nontrivial Interactions: Emergence of Cellular Automaton Dynamics

A cellular automaton (CA) is a mathematical construct invented by John von Neumann (1951) in the 1940s. CAs not only are of immense conceptual interest (laying the foundation of the field of artificial life), they also have practical applications in computer science as they are heavily used as a discretizing technique for performing complex distributed computation in, among others, statistical mechanics, fluid dynamics, and nonequilibrium phase transitions (Chopard & Droz 2005, Deutsch & Dormann 2005). However, CAs remained viewed as artificial mathematical constructs, born in the genius mind of von Neumann; i.e., CAs are useful (in computer science) and fun, but they do not actually exist in nature. Or do they? Our proposition that the quasi-hexagonal lattice of ocellated lizard colored skin scales is a living CA (Fofonjka & Milinkovitch 2021, Jahanbakhsh & Milinkovitch 2022, Manukyan et al. 2017) makes us reconsider this position.

The motivation of von Neumann in developing CAs was to define the requirements for a machine (an automaton) to not only compute but also replicate itself, without losing any of its original complexity (hence, von Neumann called it a universal constructor). It will not escape the reader's attention that this objective fundamentally pertains to uncovering the logical organization underpinning biological systems. In 1952 and 1953, von Neumann wrote a manuscript entitled "The Theory of Automata: Construction, Reproduction, Homogeneity" in which, on the basis of concepts developed in his earlier kinematic model, he developed an automaton that he

qualified to be cellular because it consists of an infinite 2D square grid of discrete elements (or so-called cells, although they are not meant to represent biological cells) that can each take any of 29 available states, such as dormant, dead, alive, and multiple transmission states (with different information transfer abilities from and to neighbors). This discretized 2D organization was personally suggested to von Neumann by Stanislaw Ulam (1952) following his own work, "Random Processes and Transformations." Starting from an initial condition, the states of all elements in a von Neumann automaton are iteratively updated using a transition rule or rule table, which defines the state of each element at iteration $i + 1$ as a function of both its own state and the states of its four nearest neighbors at iteration i (**Figure 4a**).

Astonishingly, von Neumann showed that his CA behaves as a universal Turing machine (Turing 1937) and as a universal constructor (although he noted that the former property is not necessary for the latter). Indeed, von Neumann found, without the help of a computer, a particular initial pattern of nearly 200,000 elements (a large proportion of which consists of a long tail of elements that acts as the tape interpreted by the constructor) and a rule table that jointly allow the initial pattern to reproduce itself, exactly and ad infinitum. Importantly, both the constructor and the input tape (i.e., the description of the constructor) are reproduced in the process. Von Neumann's manuscript on CA remained a draft until his death in 1957. Remarkably, von Neumann proposed these logical concepts before the discovery of real life's (biological) transcription and translation processes. Although Arthur Burks published in 1966 a careful reconstruction (von Neumann & Burks 1966) of the 29-state universal copier and constructor on the basis of von Neumann's draft manuscript and notes, the whole enterprise was validated by numerical simulations only in 1995 (Pesavento 1995) due to the insufficient computing power of earlier times. More generally, von Neumann's work on CA shows that biological processes, including reproduction, can be described algorithmically and can be achieved by machines. Later work by Edgar Codd (1968) and Christopher Langton (1984) uncovered simpler self-replicating constructors, whereas John Conway (Gardner 1970) and Stephen Wolfram (1984a,b,c, 2002) described simpler, yet Turing-complete, CAs.

But what is the relation between CAs and skin color patterning? Many species of snakes and lizards exhibit a pointillist (i.e., spatially discretized) skin color pattern consisting of the juxtaposition of scales of different colors, with each scale being monochromatic (**Figure 4b**). Although, in some species, such as the Madagascar giant day gecko (*Phelsuma grandis*), the scale-by-scale pattern is established in ovo and remains invariant after birth, other species develop their adult scale-by-scale pattern after hatching through dynamics that consist of individual scales flipping their state between two (or sometimes three) possible colors. Such state- and time-discretized dynamics seem at odd with the paradigmatic continuous (at the macroscale) RD process because the juxtaposition of skin scales (typically 0.2–5 mm in size), rather than the segregation of chromatophores (typically 10–20 μm), establishes the pattern. This process was initially investigated in the ocellated lizard (*Timon lepidus*) (**Figure 4c**) where scale color flipping generates the adult labyrinthine pattern of contrasting black and green chains of scales (Fofonjka & Milinkovitch 2021, Manukyan et al. 2017). Crucially, these patterns are not random. If they were, they would exhibit much more frequent random clumping of scales of the same color [as formally quantified by Manukyan et al. (2017)]. In other words, as we do not observe these random green or black patches of scales, one can safely conclude that the process is not scale autonomous; i.e., scales cannot have a probability of flipping color solely based on their own color. One of us (M.C.M.) then conjectured that these macroscopic patterns are dynamically computed by a stochastic extension of the von Neumann CA on a discrete-state dynamical lattice of skin scales (Manukyan et al. 2017); i.e., color flipping of each skin scale is governed by its own color and the colors of its neighbors.

We validated this conjecture by extracting the rule table of the CA from high-resolution reconstructions (Martins et al. 2015) of dorsal skin geometry and color texture of ocellated lizards at multiple time points (**Figure 4c**), from hatching to sexual maturity (occurring when lizards are 3 to 4 years old). Schematically, the probability of color switching of a given scale turned out to increase as a function of the number of its nearest neighbors that share its color (**Figure 4d**): For example, a green scale has virtually a 0% probability of switching if it is surrounded only by black neighbors, whereas it has a maximum probability of switching to the black state if it is surrounded

a **Square lattice CA** with von Neumann neighborhood

Cell (*n* states)

Two-state CA (green and black) at a given iteration

b Ibiza wall lizard (*vedrae* morph)   Argentine tegu   Gila monster   Mangrove monitor

c Ocellated lizard (*Timon lepidus*)

270 days   310 days   450 days   1,700 days

Occurrences

NN of same color

d Probability

NN of same color   NN of same color

e
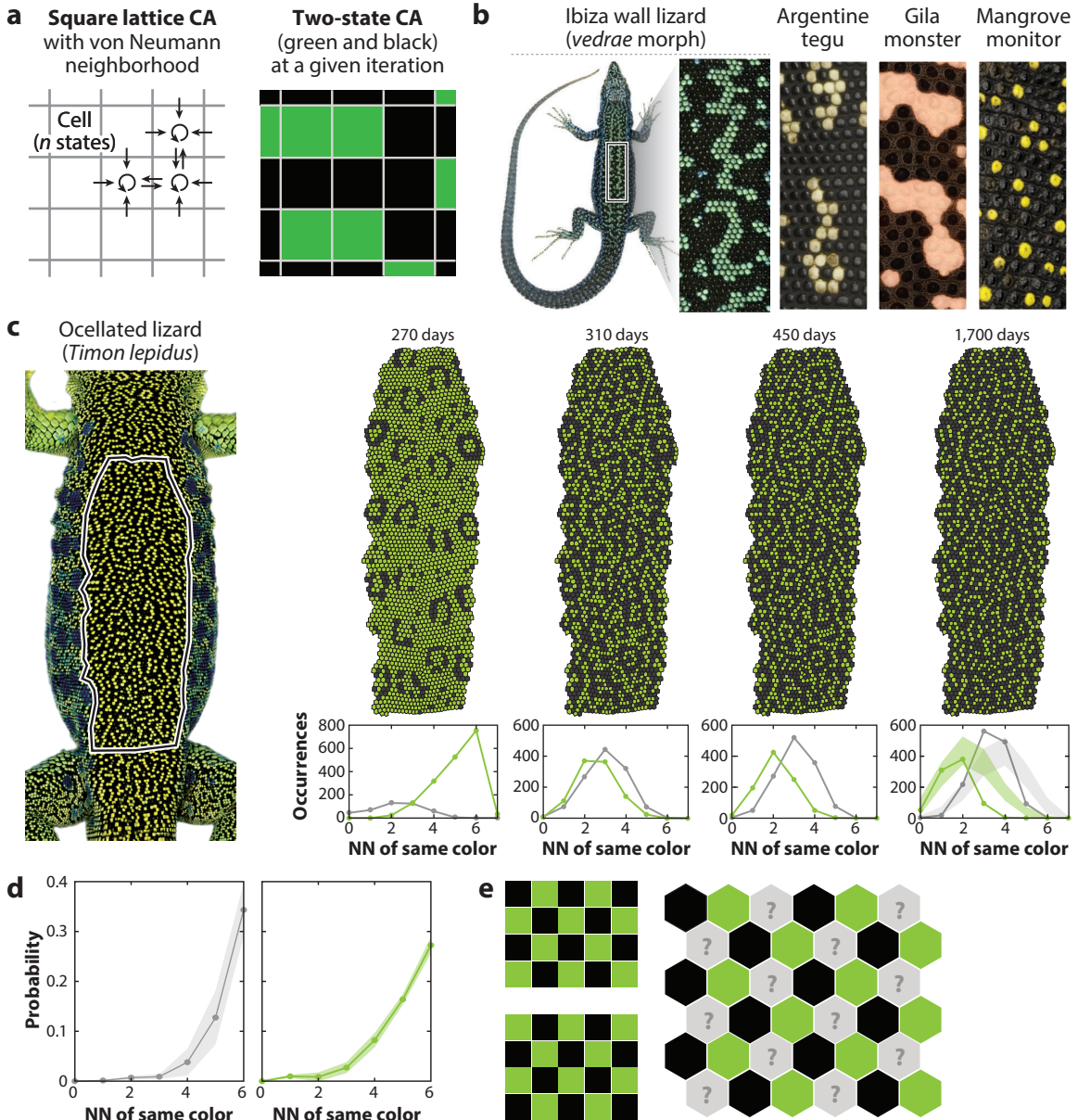
(*Caption appears on following page*)

Figure 4 (*Figure appears on preceding page*)

Lizard skin patterning and cellular automata. (*a*, *left*) So-called cells in a CA change their state at each iteration according to rules that depend on the current cell state and the current state of the four NNs (in this example, the neighborhood of the square lattice is defined according to the convention of von Neumann: north, south, east, and west). (*a*, *right*) An example of a two-state CA at a given iteration. (*b*) Details of adult skin patterns of four species of lizards exhibiting scale-by-scale patterning and color flipping dynamics. (*c*, *left*) The dorsal pattern of an adult ocellated lizard. (*c*, *right*) The skin color pattern at different time points (days posthatching are indicated). The patterns change as individual scales flip from green to black and black to green; distributions of the number of isochromatic NNs are shown below each pattern (*green* and *black* curves correspond to the statistics of green and black scales). The NN statistics for true random patterns are shown in the last time point (*shaded areas* indicate five standard deviations in a sample of 10,000 random draws). (*d*) The probabilities of flipping for black scales (*left*) and green scales (*right*) are measured (aggregated results for several individuals) and correspond to the flipping rules of a stochastic CA with two states. (*e*) Configurations in two-state (*black* and *green*) CAs where the number of NNs of the opposite color is maximized. On a square lattice (*left*), two such configurations exist, whereas, on a hexagonal lattice (*right*), multiple equivalent configurations exist: For example, in the case shown, all possible configurations, where question marks are replaced by green or black elements, are equivalent in terms of the maximization of opposite-color neighbors. Abbreviations: CA, cellular automaton; NNs, nearest neighbors.

only by green neighbors; intermediate numbers of green neighbors are associated with intermediate probabilities of color flipping. A similar relation exists for black scales: Their probabilities of switching to green increase with the number of black neighbors. The lattice of scales in real lizards is not strictly hexagonal, such that any scale can have 0–7 isochromatic scales, generating $2 \times 8 = 16$ probabilities of color switching. Because scales of the juvenile pattern have many isochromatic neighbors, the corresponding rate of color flips is high. Essentially, the CA performs a minimization of the global scale-by-scale color flip rate. For the two-state CA on the square lattice with four (north, east, south, and west) neighbors, two global minima are easily defined: the two alternative regular checkerboard patterns (see left side of **Figure 4e**). On the other hand, the hexagonal lattice is said to be "frustrated" because it is impossible for all hexagonal elements to have zero isochromatic neighbors (see right side of **Figure 4e**). Hence, the global minimization process, brought about by the CA, transforms the juvenile pattern into a labyrinthine pattern for which the rate of scale color flipping becomes small but does not vanish (**Figure 4c,d**). These CA dynamics are conveniently mapped to the simpler antiferromagnetic Lenz-Ising model (Jahanbakhsh & Milinkovitch 2022, Zakany et al. 2022).

But how is the CA generated? Surely, the CA cannot be the ultimate generative mechanism. It must emerge from lower (microscopic) spatial scales. Given the large amount of data indicating, as discussed above, that skin color patterns are produced by cell–cell interactions generating an RD dynamical system, one of us (M.C.M.) proposed that the CA emerges from the superposition of the RD dynamics with the 3D geometry of the lizard skin. Indeed, all skin scales develop prior to hatching, such that the RD patterning process in juvenile ocellated lizards occurs in a field with periodic variation of thickness (between scales and interscale skin). This, in turn, suggests that contacts between chromatophores are substantially reduced between scales, compared to contacts within scales, possibly transforming a continuous RD into a discrete CA. To test this RD-to-CA conjecture, we first performed (Manukyan et al. 2017) continuous RD numerical simulations on a 2D hexagonal lattice (with each hexagon representing the projection of a scale) (**Figure 5a**) in which we reduced all RD diffusion coefficients along the 1D edges of the hexagons (hence, edges represent interscale skin). These analyses demonstrated that such a system does indeed generate not only a scale-by-scale pattern (**Figure 5a**) but also effective CA dynamics (**Supplemental Video 4**): Color switching of individual hexagons is much faster than the overall patterning process (this is nearly equivalent to state and time discretization of a CA), and any given hexagon is essentially monochromatic at any time point (this is equivalent to the spatial discretization of a CA).

Hence, these analyses demonstrated that a CA, as a distributed computational system, is not just an abstract construct from the genius mind of von Neumann: It manifests itself upon a lizard's back

a 2D continuous RD

PD

b 3D hexagonal prisms

d

h

h_p

T

$h_p/h = 0.3$

Super-Gaussian bumps

S

h_e h_c

$$\frac{h_c}{S} = 0.5$$

$$\frac{h_e}{S} = 0.25$$

c

Growing domain of
super-Gaussian bumps

L_0

$\sqrt{2}L_0$

$2L_0$

$2\sqrt{2}L_0$
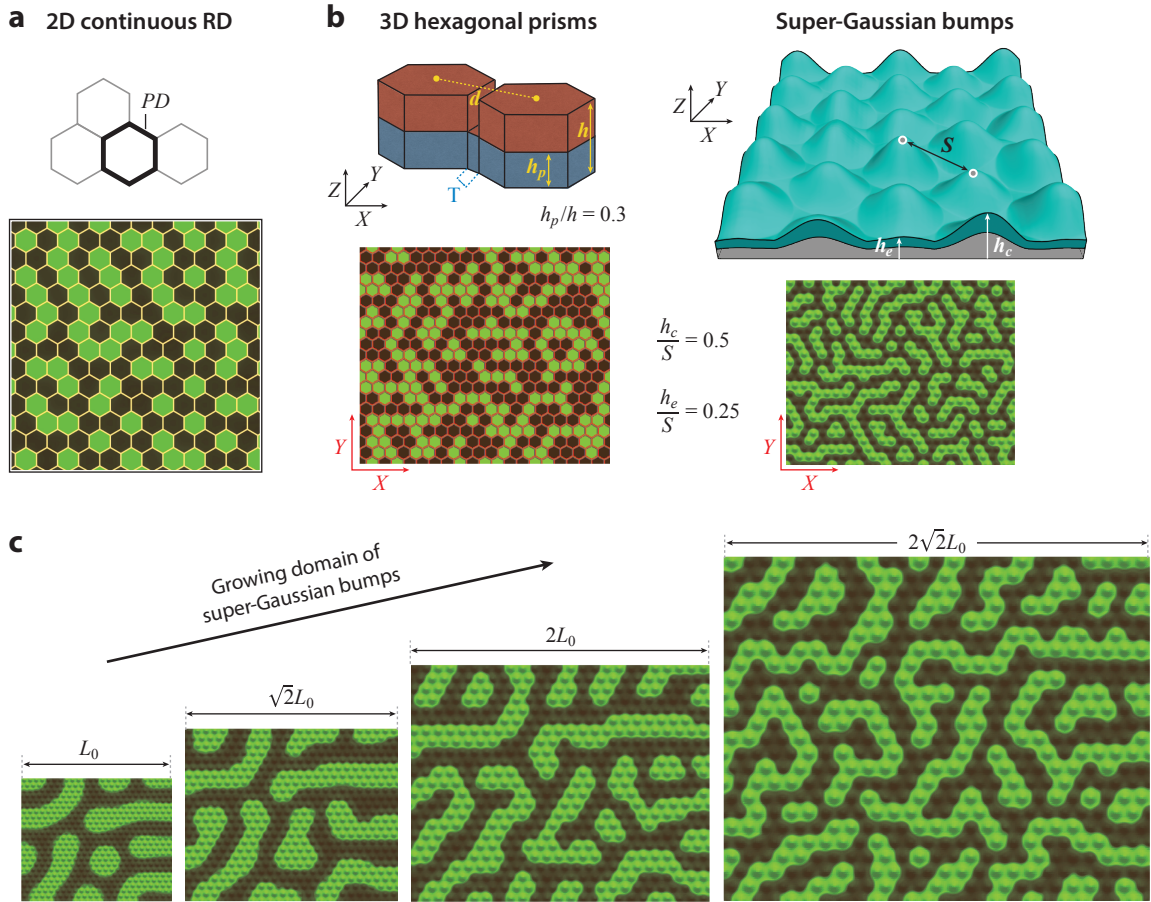
Figure 5

The geometry of scaled skin produces a CA. (*a*) The production of CA dynamics (**Supplemental Video 4**) by the 2D continuous RD model relies on the assumption that the diffusion coefficients are scaled at 1D borders of 2D polygons by a factor *P*. (*b*) Scale-by-scale color patterns and CA dynamics also emerge with homogeneous diffusion coefficients if continuous RD simulations are performed (*left*) in a 3D domain of hexagonal prisms with the domain thickness reduced at the sharp borders of the prisms (Fofonjka & Milinkovitch 2021) or (*right*) in a 3D domain made of super-Gaussian bumps mimicking the smooth transition of height at the border of scales, similar to the real skin geometry of lizards (Jahanbakhsh & Milinkovitch 2022). (*c*) Simulation in a growing domain of super-Gaussian bumps, showing the pattern at four stages corresponding to successive domain sizes isotropically increased by a factor of $\sqrt{2}$. Growth affects the scale color flipping dynamics such that the labyrinthine pattern becomes progressively more intricate because additional elements are introduced as the absolute length scale of the pattern is conserved. Readers are referred to the **Supplemental Appendices** for details on the simulations. Abbreviations: CA, cellular automaton; RD, reaction diffusion.

as a direct product of biological evolution. Importantly, Lenz-Ising, lattice Boltzmann, and CA models (among others) have been used as computational discretization techniques of continuous systems (Chopard et al. 2002, Deutsch & Dormann 2005, Wolfram 2002), including for animal pattern formation (Cocho et al. 1987a,b). However, these techniques are based on the principle that a discretized system, representing elements at the nano- or microscopic scale, can describe the continuous system at a larger spatial scale. What we describe here is fundamentally different: The discrete CA of lizard's colored skin scales emerges at the macroscopic spatial scale from the continuous RD system at the smaller spatial scale.

Given the resulting strong decoupling of RD behavior within and between scales, Stanislav Smirnov at the University of Geneva, Switzerland, proposed and derived a 2D discrete RD model on the hexagonal lattice in which diffusion is ignored (i.e., chromatophore densities are homogeneous) within scales but occurs at scale borders. In more technical terms, the model involves applying the RD equations to the triangulation of the hexagons' centers while replacing the Laplacian with its renormalized discrete counterpart (Manukyan et al. 2017). Our numerical simulations confirmed that the dynamics and probability distributions of both the continuous and discrete RD models reduce to the stochastic CA observed on the real animals (Manukyan et al. 2017). Importantly, the 2D discrete RD model constitutes a formal link between two seemingly disconnected dynamical systems: RD and CAs. We subsequently generalized the 2D discrete RD model by deriving the corresponding equations for arbitrary polygons (Jahanbakhsh & Milinkovitch 2022) to simulate color change dynamics on realistic (nonstrictly hexagonal) lattices of skin scales.

As persuasive as all these observations can be, the mapping between CAs and 2D RD models (where scales are projected on the plane in the form of polygons) must explicitly assume that the reduction of skin thickness in interscale skin justifies the scaling (by a factor P) of diffusion coefficients at the 1D borders of the polygonal scales (Manukyan et al. 2017). Although the equivalence between the factor P in two dimensions and the thickness reduction in three dimensions can be derived (Fofonjka & Milinkovitch 2021; S. Zakany & M.C. Milinkovitch, manuscript in revision), it would be more appropriate to let the CA dynamics emerge in a 3D domain with homogeneous diffusion coefficients. In other words, although 3D simulations are much more computationally intensive, they are required to let the geometry do the job without the need to introduce an ad hoc diffusion-reduction factor at scale borders. By performing continuous RD simulations in 3D lattices of hexagonal prisms, and also in 3D domains recapitulating the skin geometry of actual lizards reconstructed with episcopic microscopy (Fofonjka & Milinkovitch 2021, Jahanbakhsh & Milinkovitch 2022), we confirmed that geometry alone indeed does the job (**Figure 5b**; **Supplemental Video 5**): Scale-by-scale color patterns and CA dynamics of skin color patterning emerge from the underlying RD system.

RD numerical simulations also highlight the importance of considering growth of the domain. As discussed above, when patterning is ongoing during growth, as is the case for angelfishes, but not for zebras (because the pattern is frozen in embryos of the latter), new motifs are introduced as a direct consequence of growth; i.e., bigger angelfishes have more stripes than smaller angelfishes because the absolute distance between stripes is intrinsically set by the effective diffusion coefficients. More technically speaking, RD equations are not scale invariant (see **Supplemental Appendix 4** for details). By definition, we should observe a similar phenomenon in ocellated lizards. And, indeed, we do (Fofonjka & Milinkovitch 2021) as growth affects the scale color flipping dynamics such that the labyrinthine pattern of ocellated lizards becomes progressively more intricate (**Figure 5c**). In other words, as scales become larger but the pattern length scale must remain invariant, the absolute width (in millimeters) of green stripes does not change, but their relative width (measured in the number of scale diameters) decreases while additional, more circumvolved, stripes are introduced.

The effective space and state discretization of the ocellated lizard skin color pattern makes the patterning dynamics particularly prone to unambiguous quantitative investigation because, as the topology of the lattice does not change throughout the life of a lizard (i.e., no new scale is introduced or removed), one can unequivocally identify the position of black scales and green scales at any given time point of the dynamics. But the ocellated lizard is not an isolated idiosyncrasy: We have recently shown (Jahanbakhsh & Milinkovitch 2022) that a similar process of geometry-constrained RD can generate very different scale-by-scale macroscopic motifs in different lizard species (**Figure 4b**), such as the black and white banding of the Argentine tegu (*Salvator merianae*),

the large black and orange/pink meanders of the Gila monster (*Heloderma suspectum*), or the yellow speckles on a black background exhibited by the mangrove monitor (*Varanus indicus*). Indeed, we have shown that both a stochastic CA and a Lenz-Ising model predict neighborhood statistics of adult patterns in these species with similar efficiencies as in the ocellated lizard.

Additionally, we conjecture that other properties of skin color patterning in reptiles emerge from the presence of skin scales. For example, we propose here that reptilian scales facilitate the development of some specific motifs by their stabilization under a larger range of RD parameter values. To illustrate this effect, we search for RD parameters of the NTKK-2009 RD model that generate the large polygonal black contours characteristic of the throat and belly pattern of the perentie monitor (*Varanus giganteus*) (**Figure 6a**). We find that this stationary pattern occupies a very limited portion of the parameter space (**Figure 6b**). It could be argued that this observation makes the validity of the model suspicious (as far as the perentie monitor pattern is concerned) because fine-tuning is poorly compatible with evolutionary stability. Indeed, as genetic mutations can affect RD parameters, a pattern that is associated with a very limited range of parameter values is unlikely to evolve and/or to be easily maintained across many generations (i.e., the trait would need to be under very strong selection and/or very low mutation rates). However, we find that a much larger range of parameter values produces similar polygons but they are nonstationary: Edges move across the RD field in an ever-changing pattern until the field eventually homogenizes. In other words, the pattern is perentie-like at some time points, but it does not stabilize in time (contrary to what we assume to occur in real perentie monitors). We show here that, remarkably, a large portion of this unstable zone in parameter space readily stabilizes (and produces stationary perentie patterns) when periodic variation of the skin thickness is introduced in the form of skin scales (**Figure 6c**). Hence, we propose that the presence of scales in squamate reptiles makes some stationary patterns more likely to evolve and more robust against mutational noise. Alternatively, one could argue that the perentie pattern is nonstationary but it becomes frozen at some point during development (as discussed above for zebras). However, we do not favor, a priori, this alternative explanation because it would make the existence of the pattern sensitive to variation of the time of freezing.

2.5. Reaction Diffusion Predicts the Positions of Dark and Light Scales in Lizards

The description of the skin color patterning of the ocellated lizard, the Argentine tegu, the Gila monster, the mangrove monitor, and many other species as a stochastic CA captures three essential features: the spatial discretization of the pattern, as well as the time and state near discretization of the dynamics. However, the underlying RD process is clearly continuous in time: Scale color switching is fast but not instantaneous. Hence, the approximation brought about by state discretization might be a source of the stochastic character of the CA derived from the observations of color patterning in real lizards. In other words, one could argue that the deterministic and continuous-state RD framework might capture some scale-by-scale skin color patterning features better than the stochastic discrete-state CA and Lenz-Ising models. We have seen above that this is not the case for general statistical features of the pattern: RD, CAs, and the Lenz-Ising model all predict with very similar efficiencies the neighborhood distributions of very different steady-state patterns observed in different species.

On the other hand, because RD (*a*) implicitly integrates (whereas CA and Lenz-Ising models do not) a relation between the pattern and growth and (*b*) can exploit the continuous-state distribution of scale colors both at the initial condition and during patterning, RD might better predict the exact positions of black and of green/yellow scales in specific individuals for which the initial condition (juvenile pattern) has been recorded. Such an ambition might sound unreasonable because
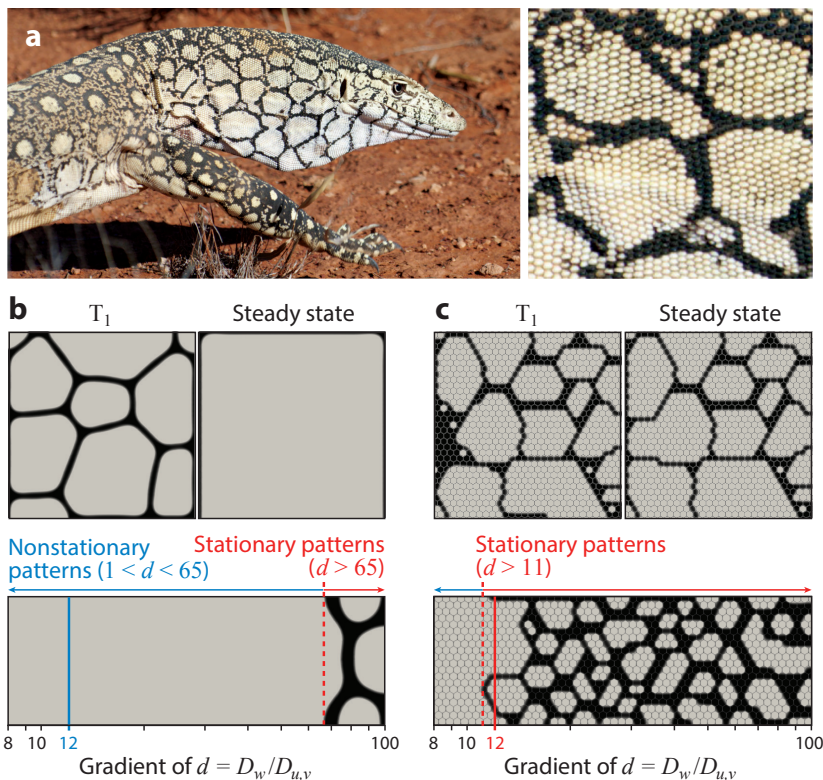
Figure 6

The skin pattern of perentie monitors is likely stabilized by the presence of scales. (*a*) Perentie monitors (*Varanus giganteus*) exhibit large polygonal black contours on their throat and belly. The magnified image on the right shows that the pattern is discretized scale by scale. (*b, top*) Two snapshots from simulation of the NTKK-2009 RD model with diffusion coefficient ratio $d = D_w/D_{u,v} = 12$. Transient perentie-like patterns (snapshot T_1) emerge, but they are not stationary and disappear at steady state. (*b, bottom*) Transient and stationary patterns obtained with continuous RD in two dimensions when varying the diffusion coefficient ratio d (logarithmic scale): Stationary patterns are obtained only for $d > 65$ (*red arrow*), whereas nonstationary patterns are obtained for $d < 65$ (*blue arrow*); hence, no stationary pattern is obtained for $d = 12$ (*blue line*), i.e., the value used at the top. (*c*) Same continuous RD simulations as in panel *b* but with a superimposed hexagonal lattice of scales, and diffusion coefficients are scaled by $P = 0.15$ at scale borders. In that case, stationary steady-state perentie-like patterns emerge for a much larger range of d (*red arrow*), including for $d = 12$, i.e., the value used at the top. Nonstationary patterns are obtained for $d < 11$ (*blue arrow*). Readers are referred to the **Supplemental Appendices** for simulation details. Abbreviation: RD, reaction diffusion.

many of the underlying cellular and molecular variables are ignored in the phenomenological RD model. Yet, we previously revealed (Jahanbakhsh & Milinkovitch 2022) that continuous-state color measured in real individual juvenile lizards indeed allows us to predict the corresponding adult patterns much better with RD (mean residual scale-by-scale error of 23.6% in ocellated lizards) than with CA or Lenz-Ising models (mean residual error of 38.9%). Further analyses indicated that, because not all scales are identical in geometry, one-third of the RD residual unpredictability is caused by skin geometry variation. Indeed, when the standard deviations of thickness, both among scales and among scale borders, measured in real lizards with episcopic microscopy, are introduced in 3D RD simulations, the mean unexplained residual unpredictability of real individual scale-by-scale patterns by RD falls to 15.1% (Jahanbakhsh & Milinkovitch 2022).

We then reasoned that the most likely remaining source of unpredictability corresponds to the sensitivity of the nonlinear dynamical system to initial conditions: Initial uncertainties of color measurements (transferred to the space of RD component concentrations using an appropriate transformation matrix) in a juvenile are likely to grow as an RD simulation of the patterning process progresses in time. To quantitatively assess this effect, we used Lyapunov spectrum analyses to compute the expected scale-by-scale error at the adult stage given a range of arbitrary uncertainties at the initial condition (Jahanbakhsh & Milinkovitch 2022). We then judged that the decision to define the color of a scale (from high-resolution color pictures) as the mean among pixels within that scale is arbitrary. We then identified that using the mode, the median, or the mean among the pixels within each juvenile scale yields colors that are indistinguishable by eye, yet the differences between these values generate a mean scale-by-scale error in the adult of 16.1%, therefore explaining most, if not all, of the 15.1% mean residual unpredictability of the actual adult lizard patterns. Note that residual unpredictability is not sensitive to fine-tuning of the RD model parameter values: Perturbing these values generates much smaller mean scale-by-scale errors than uncertainties in skin geometry and in juvenile colors (Jahanbakhsh & Milinkovitch 2022). Remarkably, these results in ocellated lizards can be generalized to the Argentine black and white tegu, the Gila monster, and the mangrove monitor: The mean residual error in each of these species is explained by a combination of uncertainty in the spatial distribution of skin thickness and in color measurement at the initial condition (Jahanbakhsh & Milinkovitch 2022). Hence, the phenomenological deterministic RD model itself is not the source of the residual error: It does generate high predictability of dark and light scale positions in individual adult patterns, without the need to parameterize the system down to its many cellular and molecular variables.

2.6. Phenomenological Reaction-Diffusion Models Are Unreasonably Robust

Possibly the most frequent criticism toward the use of effective phenomenological models is that they are necessarily wrong in the sense that they ignore much of the underlying molecular details. However, this is an ill-defined criticism. Indeed, such an argument would make wrong any scientific hypothesis ignoring the smallest spatial and temporal scales. After all, nobody seriously challenges cell biology or molecular biology approaches because they ignore quantum mechanics, despite the efficiency and relevancy of this framework at very small spatial scales. The important question for evaluating the efficiency of any model/theory is how robustly it predicts observations. If the topic of interest lies in understanding the meso- and macroscopic skin color patterning process in vertebrates, we can safely consider that RD is very, possibly "unreasonably," efficient and robust at multiple levels. First, as discussed above, the NTKK-2009 RD model developed to predict skin color patterns in wild-type and mutant zebrafishes (Nakamasu et al. 2009) captures most of the underlying dynamical processes shared among vertebrates (and possibly beyond) such that it also predicts the CA-like scale-by-scale color patterning of the skin in multiple lizard species when it is combined with the periodic variation of skin thickness introduced by skin scales in multiple species of lizards (Fofonjka & Milinkovitch 2021, Jahanbakhsh & Milinkovitch 2022, Manukyan et al. 2017). Second, as far as the discretized dynamics observed in lizard skin color patterning is concerned, not only the unmanageable profusion of variables at the nanoscopic and microscopic scales but also the specificities of the NTKK-2009 model become irrelevant. Indeed, snapping of the pattern to the borders of the scales and the CA-like behavior are robust to very large variations of the model as they both occur irrespective of the system of nonlinear PDEs that is used (Fofonjka & Milinkovitch 2021). Third, the emergence of a CA behavior is also robust to alterations of the real skin geometry (Fofonjka & Milinkovitch 2021, Jahanbakhsh & Milinkovitch 2022): A transition between continuous and discrete patterns is triggered in basically any 3D lattice where some nontrivial reduction of skin thickness occurs at scale boundaries. These second

and third points indicate that the effect of 3D geometry on pattern formation is likely to be very general.

Finally, a model/theory is particularly useful if it can robustly predict unknown results attainable through experiments. Such a case recently occurred during our investigations of scale-by-scale RD patterning. Although we always assumed that such a process generates only two discrete states (e.g., green and black in ocellated lizards), numerical simulations on the regular hexagonal lattice unexpectedly identified steady-state subclusters in color distribution within the two large clusters of green and black scales (S. Zakany & M.C. Milinkovitch, manuscript in revision). The differences of greenness or blackness (expressed in RD component densities) between scales belonging to different green or black subclusters are typically small, but they are unambiguously defined by the general state (green or black) of the scales' nearest neighbors; i.e., green scales surrounded by zero, one, two, three, four, five, or six green neighbors exhibit distinct (nonoverlapping) values of green. Similarly, seven levels of black are associated with black scales surrounded by zero to six black scales. Again, the relevant question is whether this feature (subclustering) is an oddity specific to the RD model (hence, has no relevance with the real biological patterning system), or whether it reflects an undetected reality. As real lizards do not exhibit a perfectly regular hexagonal lattice of scales, we first evaluated if the dependence of color on the number of isochromatic nearest neighbors would stand in lattices where the hexagon centers are randomly displaced with various levels of noise. These analyses indicated that the greenness of a green scale, or the blackness of a black scale, strongly correlates with $\mathcal{L}_k$, i.e., the sum of side lengths $L_{k\tilde{k}}$ that the polygonal scale k shares with its first-neighbor polygons $\tilde{k}$ of the same general color (green or black) (S. Zakany & M.C. Milinkovitch, manuscript in revision). As a consequence, the correlation between the color of scales and their neighborhood configuration is maintained in perturbed lattices (even in quasi-hexagonal networks of skin scales reconstructed from real ocellated lizards), but the subclusters increasingly overlap as the noise in the positions of polygon centers is made larger. The color subclustering phenomenon occurs with continuous and discrete RD models as well as in bona fide 3D domains of skin scales. Similar to the robustness of the scale-by-scale CA dynamics discussed above, subclustering is robust to very large modifications of the RD model and even occurs in one-component models with nonlinear competition between two stable steady states (S. Zakany & M.C. Milinkovitch, manuscript in revision).

To assess whether such subclustering occurs in actual lizards, we analyzed the colors of individual scales with hyperspectral imaging in adult ocellated lizards and revealed that subtle neighborhood-dependent color subclustering (not visible with the naked eye) is indeed present in these animals (S. Zakany & M.C. Milinkovitch, manuscript in revision). Confirming in real animals this nontrivial prediction of the numerical model demonstrates, as for the prediction of the CA dynamics, that phenomenological RD models robustly capture relevant underlying dynamics. Possibly even more surprising is the ability of these models to capture features that can be identified at the cellular scale. Indeed, using histological serial sections, we have shown that the positions of melanophores within a given scale correlate with (*a*) the corresponding numerically predicted color subcluster of that scale, hence (*b*) the number of its isochromatic neighbors. In conclusion, irrespective of their form, discretization, and spatial dimensionality, phenomenological RD models are unreasonably robust in predicting some specific features of the dynamical self-organization system, such as CA dynamics, as well as much more subtle color subclustering.

3. CONCLUSIONS

Given the data available to date, the "unreasonable effectiveness of RD" becomes less surprising for the following five reasons. First, all experimental results strongly support the notion that

skin color patterning in vertebrates is a self-organized process; i.e., skin patterns autonomously emerge from specific interactions among the chromatophores themselves. These interactions have been shown to affect cell-specific processes such as migration/dispersal, survival, proliferation, and differentiation. Second, the presence of short- and long-range cell–cell interactions (the latter occurring via long thin cell projections) is effectively equivalent to slow- and fast-diffusing morphogens, making the RD mathematical framework appropriate. Third, patterning of skin colors does not seem to involve any dominating mechanical component. This must be contrasted with multiple mechano-chemical morphogenetic processes (Ho et al. 2019, Stooke-Vaughan & Campàs 2018) that cannot be effectively described with RD alone. Fourth, although the underlying molecular and cellular dynamics occur at the nano- and microscopic scales, the trait of interest (skin color patterns) and its dynamics of development occur at the meso- or macroscale. A continuous deterministic model such as RD is therefore pertinent because it describes how averages of chromatophore densities vary at the macroscopic scale (as discussed in detail in **Supplemental Appendix 5**). Fifth, growth can readily be integrated into RD models (Fofonjka & Milinkovitch 2021, Jahanbakhsh & Milinkovitch 2022). Indeed, as RD implicitly integrates a relation between the pattern absolute length scale and the size of the domain in which it occurs, this mathematical framework allows the effective recapitulation of skin color pattern dynamics that usually do not scale as body size increases. We, however, also discussed the fact that mechanisms appropriately scaling reaction parameters may generate scaling Turing patterns (Ishihara & Kaneko 2006). Hence, we conclude that RD systems can indeed capture most of the functionally relevant behavior of skin color patterning without the need to parameterize the unmanageable profusion of variables at the nanoscopic and microscopic scales (Milinkovitch 2021).

DISCLOSURE STATEMENT

ACKNOWLEDGMENTS

LITERATURE CITED

Aguilar-Hidalgo D, Werner S, Wartlick O, Gonzalez-Gaitan M, Friedrich BM, Julicher F. 2018. Critical point in self-organized tissue growth. *Phys. Rev. Lett.* 120:198102

Bagnara JT, Matsumoto J. 2006. Comparative anatomy and physiology of pigment cells in nonmammalian tissues. In *The Pigmentary System: Physiology and Pathophysiology*, ed. JJ Nordlund, RE Boissy, VJ Hearing, RA King, WS Oetting, JP Ortonne, pp. 11–59. Malden, MA: Blackwell

Baker RE, Schnell S, Maini PK. 2006a. A clock and wavefront mechanism for somite formation. *Dev. Biol.* 293:116–26

Baker RE, Schnell S, Maini PK. 2006b. A mathematical investigation of a clock and wavefront model for somitogenesis. *J. Math. Biol.* 52:458–82

Bard JBL. 1977. Unity underlying different zebra striping patterns. *J. Zool.* 183:527–39

Barkai N, Ben-Zvi D. 2009. 'Big frog, small frog'–maintaining proportions in embryonic development: delivered on 2 July 2008 at the 33rd FEBS congress in Athens, Greece. *FEBS J.* 276:1196–207

Bottriell LG. 1987. *King Cheetah: The Story of the Quest*. New York: Brill

Budi EH, Patterson LB, Parichy DM. 2008. Embryonic requirements for ErbB signaling in neural crest development and adult pigment pattern formation. *Development* 135:2603–14

Čapek D, Müller P. 2019. Positional information and tissue scaling during development and regeneration. *Development* 146:dev177709

Chopard B, Droz M. 2005. *Cellular Automata Modeling of Physical Systems*. New York: Cambridge Univ. Press

Chopard B, Dupuis A, Masselot A, Luthi P. 2002. Cellular automata and lattice Boltzmann techniques: an approach to model and simulate complex systems. *Adv. Complex Syst.* 5:103–246

Cocho G, Perez-Pascual R, Rius JL. 1987a. Discrete systems, cell-cell interactions and color pattern of animals. I. Conflicting dynamics and pattern formation. *J. Theor. Biol.* 125:419–35

Cocho G, Perez-Pascual R, Rius JL, Soto F. 1987b. Discrete systems, cell-cell interactions and color pattern of animals. II. Clonal theory and cellular automata. *J. Theor. Biol.* 125:437–47

Codd EF. 1968. *Cellular Automata*. New York: Academic

Cooke J, Zeeman EC. 1976. A clock and wavefront model for control of the number of repeated structures during animal morphogenesis. *J. Theor. Biol.* 58:455–76

Cotterell J, Robert-Moreno A, Sharpe J. 2015. A local, self-organizing reaction-diffusion model can explain somite patterning in embryos. *Cell Syst.* 1:257–69

Cross MC, Hohenberg PC. 1993. Pattern formation outside of equilibrium. *Rev. Mod. Phys.* 65:851–1112

Deutsch A, Dormann S. 2005. *Cellular Automaton Modeling of Biological Pattern Formation: Characterization, Applications, and Analysis*. Boston: Birkhäuser

Dooley CM, Mongera A, Walderich B, Nüsslein-Volhard C. 2013. On the embryonic origin of adult melanophores: the role of ErbB and Kit signalling in establishing melanophore stem cells in zebrafish. *Development* 140:1003–13

Eom DS, Bain EJ, Patterson LB, Grout ME, Parichy DM. 2015. Long-distance communication by specialized cellular projections during pigment pattern development and evolution. *eLife* 4:e12401

Eom DS, Inoue S, Patterson LB, Gordon TN, Slingwine R, et al. 2012. Melanophore migration and survival during zebrafish adult pigment stripe development require the immunoglobulin superfamily adhesion molecule Igsf11. *PLOS Genet.* 8:e1002899

Eom DS, Parichy DM. 2017. A macrophage relay for long-distance signaling during postembryonic tissue remodeling. *Science* 355:1317–19

Epperlein HH, Claviez M. 1982. Formation of pigment cell patterns in *Triturus alpestris* embryos. *Dev. Biol.* 91:497–502

Epperlein HH, Lofberg J, Olsson L. 1996. Neural crest cell migration and pigment pattern formation in urodele amphibians. *Int. J. Dev. Biol.* 40:229–38

Epstein IR, Xu B. 2016. Reaction-diffusion processes at the nano- and microscales. *Nat. Nanotechnol.* 11:312–19

Fisher RA. 1937. The wave of advance of advantageous genes. *Ann. Eugen.* 7:355–69

Fofonjka A, Milinkovitch MC. 2021. Reaction-diffusion in a growing 3D domain of skin scales generates a discrete cellular automaton. *Nat. Commun.* 12:2433

Frohnhofer HG, Krauss J, Maischein HM, Nüsslein-Volhard C. 2013. Iridophores and their interactions with other chromatophores are required for stripe formation in zebrafish. *Development* 140:2997–3007

Gardner M. 1970. The fantastic combinations of John Conway's new solitaire game "life." *Sci. Am.* 223:120–23

Gierer A, Meinhardt H. 1972. A theory of biological pattern formation. *Kybernetik* 12:30–39

Green JB, Sharpe J. 2015. Positional information and reaction-diffusion: Two big ideas in developmental biology combine. *Development* 142:1203–11

Hamada H, Watanabe M, Lau HE, Nishida T, Hasegawa T, et al. 2014. Involvement of Delta/Notch signaling in zebrafish adult pigment stripe patterning. *Development* 141:318–24

Haupaix N, Curantz C, Bailleul R, Beck S, Robic A, Manceau M. 2018. The periodic coloration in birds forms through a prepattern of somite origin. *Science* 361:eaar4777

Haupaix N, Manceau M. 2020. The embryonic origin of periodic color patterns. *Dev. Biol.* 460:70–76

Ho WKW, Freem L, Zhao D, Painter KJ, Woolley TE, et al. 2019. Feather arrays are patterned by interacting signalling and cell density waves. *PLOS Biol.* 17:e3000132

Inaba M, Yamanaka H, Kondo S. 2012. Pigment pattern formation by contact-dependent depolarization. *Science* 335:677

Ishihara S, Kaneko K. 2006. Turing pattern with proportion preservation. *J. Theor. Biol.* 238:683–93

Ising E. 1925. Beitrag zur Theorie des Ferromagnetismus. *Z. Phys.* 31:253–58

Jahanbakhsh E, Milinkovitch MC. 2022. Modeling convergent scale-by-scale skin color patterning in multiple species of lizards. *Curr. Biol.* 32:5069–82.e13

Kolmogorov A, Petrovskii I, Piskunov N. 1937. Study of the diffusion equation with growth of the quantity of matter and its application to a biological problem. *Bull. Mosc. Univ.* 1:1–25

Kondo S, Asal R. 1995. A reaction-diffusion wave on the skin of the marine angelfish *Pomacanthus*. *Nature* 376:765–68

Kondo S, Miura T. 2010. Reaction-diffusion model as a framework for understanding biological pattern formation. *Science* 329:1616–20

Kondo S, Watanabe M, Miyazawa S. 2021. Studies of Turing pattern formation in zebrafish skin. *Philos. Trans. R. Soc. A* 379:20200274

Kronforst MR, Barsh GS, Kopp A, Mallet J, Monteiro A, et al. 2012. Unraveling the thread of nature's tapestry: the genetics of diversity and convergence in animal pigmentation. *Pigment Cell Melanoma Res.* 25:411–33

Kuriyama T, Miyaji K, Sugimoto M, Hasegawa M. 2006. Ultrastructure of the dermal chromatophores in a lizard (Scincidae: *Plestiodon latiscutatus*) with conspicuous body and tail coloration. *Zool. Sci.* 23:793–99

Langton CG. 1984. Self-reproduction in cellular automata. *Physica D* 10:135–44

Larison B, Kaelin CB, Harrigan R, Henegar C, Rubenstein DI, et al. 2021. Population structure, inbreeding and stripe pattern abnormalities in plains zebras. *Mol. Ecol.* 30:379–90

Lenz W. 1920. Beiträge zum Verständnis der magnetischen Erscheinungen in festen Körpern. *Phys. Z.* 21:613–15

Lorenz EN. 1963. Deterministic nonperiodic flow. *J. Atmos. Sci.* 20:130–41

Macmillan GJ. 1976. Melanoblast-tissue interactions and the development of pigment pattern in *Xenopus* larvae. *J. Embryol. Exp. Morphol.* 35:463–84

Maderspacher F, Nüsslein-Volhard C. 2003. Formation of the adult pigment pattern in zebrafish requires leopard and obelix dependent cell interactions. *Development* 130:3447–57

Mahalwar P, Walderich B, Singh AP, Nüsslein-Volhard C. 2014. Local reorganization of xanthophores fine-tunes and colors the striped pattern of zebrafish. *Science* 345:1362–64

Manukyan L, Montandon SA, Fofonjka A, Smirnov S, Milinkovitch MC. 2017. A living mesoscopic cellular automaton made of skin scales. *Nature* 544:173–79

Marcon L, Diego X, Sharpe J, Müller P. 2016. High-throughput mathematical analysis identifies Turing networks for patterning with equally diffusing signals. *eLife* 5:e14022

Martins AF, Bessant M, Manukyan L, Milinkovitch MC. 2015. R^{2}OBBIE-3D, a fast robotic high-resolution system for quantitative phenotyping of surface geometry and colour-texture. *PLOS ONE* 10:e0126740

Mateus R, Holtzer L, Seum C, Hadjivasiliou Z, Dubois M, et al. 2020. BMP signaling gradient scaling in the zebrafish pectoral fin. *Cell Rep.* 30:4292–302.e7

Meinhardt H. 1982. *Models of Biological Pattern Formation*. New York: Academic

Meinhardt H, Gierer A. 1974. Applications of a theory of biological pattern formation based on lateral inhibition. *J. Cell Sci.* 15:321–46

Milinkovitch MC. 2021. Emergence of self-organizational patterning at the mesoscopic scale. *Dev. Cell* 56:719–21

Milinkovitch MC, Tzika A. 2007. Escaping the mouse trap: the selection of new Evo-Devo model species. *J. Exp. Zool. B Mol. Dev. Evol.* 308:337–46

Miyazawa S. 2020. Pattern blending enriches the diversity of animal colorations. *Sci. Adv.* 6:eabb9107

Miyazawa S, Okamoto M, Kondo S. 2010. Blending of animal colour patterns by hybridization. *Nat. Commun.* 1:66

Murray JD. 1980. A pattern formation mechanism and its application to mammalian coat markings. In *Vito Volterra Symposium on Mathematical Models in Biology*, ed. C Barigozzi, pp. 360–99. Berlin: Springer

Murray JD. 1981a. On pattern formation mechanisms for lepidopteran wing patterns and mammalian coat markings. *Philos. Trans. R. Soc. Lond. B Biol. Sci.* 295:473–96

Murray JD. 1981b. A pre-pattern formation mechanism for animal coat markings. *J. Theor. Biol.* 88:161–99

Murray JD. 2003. *Mathematical Biology II: Spatial Models and Biomedical Applications*. New York: Springer. 3rd ed.

Nakamasu A, Takahashi G, Kanbe A, Kondo S. 2009. Interactions between zebrafish pigment cells responsible for the generation of Turing patterns. *PNAS* 106:8429–34

Nüsslein-Volhard C. 1994. Of flies and fishes. *Science* 266:572–74

Olsson M, Stuart-Fox D, Ballen C. 2013. Genetics and evolution of colour patterns in reptiles. *Semin. Cell Dev. Biol.* 24:529–41

Owen JP, Kelsh RN, Yates CA. 2020. A quantitative modelling approach to zebrafish pigment pattern formation. *eLife* 9:e52998

Parichy DM. 1996. When neural crest and placodes collide: interactions between melanophores and the lateral lines that generate stripes in the salamander *Ambystoma tigrinum tigrinum* (Ambystomatidae). *Dev. Biol.* 175:283–300

Parichy DM. 2003. Pigment patterns: fish in stripes and spots. *Curr. Biol.* 13:R947–50

Parichy DM, Turner JM. 2003. Temporal and cellular requirements for Fms signaling during zebrafish adult pigment pattern development. *Development* 130:817–33

Patterson LB, Bain EJ, Parichy DM. 2014. Pigment cell interactions and differential xanthophore recruitment underlying zebrafish stripe reiteration and *Danio* pattern evolution. *Nat. Commun.* 5:5299

Patterson LB, Parichy DM. 2013. Interactions with iridophores and the tissue environment required for patterning melanophores and xanthophores during zebrafish adult pigment stripe formation. *PLOS Genet.* 9:e1003561

Patterson LB, Parichy DM. 2019. Zebrafish pigment pattern formation: insights into the development and evolution of adult form. *Annu. Rev. Genet.* 53:505–30

Pesavento U. 1995. An implementation of von Neumann's self-reproducing machine. *Artif. Life* 2:337–54

Prigogine I. 1955. *Introduction to Thermodynamics of Irreversible Processes*. Springfield, IL: C. Thomas. 3rd ed.

Protas ME, Patel NH. 2008. Evolution of coloration patterns. *Annu. Rev. Cell Dev. Biol.* 24:425–46

Richmond DL, Oates AC. 2012. The segmentation clock: inherited trait or universal design principle? *Curr. Opin. Genet. Dev.* 22:600–6

Romanova-Michaelides M, Hadjivasiliou Z, Aguilar-Hidalgo D, Basagiannis D, Seum C, et al. 2022. Morphogen gradient scaling by recycling of intracellular Dpp. *Nature* 602:287–93

Saenko SV, Teyssier J, van der Marel D, Milinkovitch MC. 2013. Precise colocalization of interacting structural and pigmentary elements generates extensive color pattern variation in *Phelsuma* lizards. *BMC Biol.* 11:105

Schweisguth F, Corson F. 2019. Self-organization in pattern formation. *Dev. Cell* 49:659–77

Singh AP, Nüsslein-Volhard C. 2015. Zebrafish stripes as a model for vertebrate colour pattern formation. *Curr. Biol.* 25:R81–92

Singh AP, Schach U, Nüsslein-Volhard C. 2014. Proliferation, dispersal and patterned aggregation of iridophores in the skin prefigure striped colouration of zebrafish. *Nat. Cell Biol.* 16:607–14

Soroldoni D, Jörg DJ, Morelli LG, Richmond DL, Schindelin J, et al. 2014. A Doppler effect in embryonic pattern formation. *Science* 345:222–25

Stooke-Vaughan GA, Campàs O. 2018. Physical control of tissue morphogenesis across scales. *Curr. Opin. Genet. Dev.* 51:111–19

Streisinger G, Walker C, Dower N, Knauber D, Singer F. 1981. Production of clones of homozygous diploid zebra fish (*Brachydanio rerio*). *Nature* 291:293–96

Stuart-Fox D, Moussalli A. 2008. Selection for social signalling drives the evolution of chameleon colour change. *PLOS Biol.* 6:e25

Suzuki N, Hirata M, Kondo S. 2003. Traveling stripes on the skin of a mutant mouse. *PNAS* 100:9680–85

Teyssier J, Saenko SV, van der Marel D, Milinkovitch MC. 2015. Photonic crystals cause active colour change in chameleons. *Nat. Commun.* 6:6368

Turing AM. 1937. On computable numbers, with an application to the Entscheidungsproblem. *Proc. Lond. Math. Soc.* s2-42:230–65

Turing AM. 1952. The chemical basis of morphogenesis. *Philos. Trans. R. Soc. Lond. Ser. B Biol. Sci.* 237:37–72

Twitty VC. 1945. The developmental analysis of specific pigment patterns. *J. Exp. Zool.* 100:141–78

Tzika A, Milinkovitch MC. 2008. A pragmatic approach for selecting evo-devo model species in amniotes. In *Evolving Pathways: Key Themes in Evolutionary Developmental Biology*, ed. A Minelli, G Fusco, pp. 119–40. Cambridge, UK: Cambridge Univ. Press

Tzika AC, Ullate-Agote A, Zakany S, Kummrow M, Milinkovitch MC. 2023. Somitic positional information guides self-organised patterning of snake scales. *Sci. Adv.* 9:eadf8834

Ulam S. 1952. Random processes and transformations. In *Proceedings of the International Congress of Mathematicians: Cambridge, Massachusetts, U.S.A.: August 30–September 6, 1950*, Vol. 2, ed. LM Graves, PA Smith, E Hille, O Zariski, pp. 264–75. Providence, RI: Am. Math. Soc.

Ullate-Agote A, Burgelin I, Debry A, Langrez C, Montange F, et al. 2020. Genome mapping of a LYST mutation in corn snakes indicates that vertebrate chromatophore vesicles are lysosome-related organelles. *PNAS* 117:26307–17

Vasilopoulos G, Painter KJ. 2016. Pattern formation in discrete cell tissues under long range filopodia-based direct cell to cell contact. *Math. Biosci.* 273:1–15

Volkening A, Sandstede B. 2018. Iridophores as a source of robustness in zebrafish stripes and variability in *Danio* patterns. *Nat. Commun.* 9:3231

von Neumann J. 1951. The general and logical theory of automata. In *Cerebral Mechanisms in Behavior: The Hixon Symposium*, ed. LA Jeffress, pp. 288–326. New York: Wiley

von Neumann J, Burks AW. 1966. *The Theory of Self-Reproducing Automata*. Champaign: Univ. Illinois Press

Wang S, Garcia-Ojalvo J, Elowitz MB. 2022. Periodic spatial patterning with a single morphogen. *Cell Syst.* 13:1033–47.e7

Wartlick O, Mumcu P, Kicheva A, Bittig T, Seum C, et al. 2011. Dynamics of Dpp signaling and proliferation control. *Science* 331:1154–59

Watanabe M, Kondo S. 2012. Changing clothes easily: connexin41.8 regulates skin pattern variation. *Pigment Cell Melanoma Res.* 25:326–30

Watanabe M, Kondo S. 2015. Comment on "Local reorganization of xanthophores fine-tunes and colors the striped pattern of zebrafish." *Science* 348:297

Wigner EP. 1960. The unreasonable effectiveness of mathematics in the natural sciences. *Commun. Pure Appl. Math.* 13:1–14

Wolfram S. 1984a. Cellular automata as models of complexity. *Nature* 311:419–24

Wolfram S. 1984b. Computation theory of cellular automata. *Commun. Math. Phys.* 96:15–57

Wolfram S. 1984c. Universality and complexity in cellular automata. *Physica D* 10(1–2):1–35

Wolfram S. 2002. *A New Kind of Science*. Champaign, IL: Wolfram Media

Wolpert L. 1969. Positional information and the spatial pattern of cellular differentiation. *J. Theor. Biol.* 25:1–47

Wolpert L. 1971. Positional information and pattern formation. *Curr. Top. Dev. Biol.* 6:183–224

Yamaguchi M, Yoshimoto E, Kondo S. 2007. Pattern regulation in the stripe of zebrafish suggests an underlying dynamic and autonomous mechanism. *PNAS* 104:4790–93

Yamanaka H, Kondo S. 2014. In vitro analysis suggests that difference in cell movement during direct interaction can generate various pigment patterns in vivo. *PNAS* 111:1867–72

Zakany S, Smirnov S, Milinkovitch MC. 2022. Lizard skin patterns and the Ising model. *Phys. Rev. Lett.* 128:048102